5.0 CONCLUSIONS AND APPLICATION OF SCALING STUDIES

This section provides the conclusions of the report, the comparison of AP600 and AP1000 PIRT, as well as a discussion of the application of results of the AP1000 scaling studies.

5.1 CONCLUSIONS

The purpose of this report is to provide the information necessary for the NRC to decide whether the AP600 test programs are sufficient to meet the requirements of 10 CFR Part 52 for an application for Design Certification for an AP1000. In Reference 1, Westinghouse presented a description of the AP1000 that contrasted the design of the AP600 and AP1000.

In Section 2 of this report, the AP1000 PIRT are presented. These PIRT were developed by Westinghouse and non-Westinghouse experts in the areas of thermal-hydraulics and AP600 passive system performance characteristics. These PIRT are presented and compared to the AP600 PIRT.

Four PIRT were developed for AP1000:

- Large-Break LOCA
- Small-Break LOCA/Long Term Cooling
- Non-LOCA
- Containment

The AP1000 PIRT are very similar to the AP600 PIRT with the most significant difference being the potential higher importance of hot leg entrainment during the post-ADS-4 actuation phases of the small break LOCA accidents. Therefore, scaling of these phases of the transient are of particular interest for the AP1000.

An overview description of the AP600 tests is provided in Section 3 of this report. For each test, a conclusion is made regarding the applicability of the test and/or test data to the AP1000. The major conclusion for this section is that the tests performed for AP600 bound the expected conditions for the AP1000. In addition, the NRC-sponsored confirmatory tests at ROSA and OSU are also useful in providing test data for the AP1000.

In Section 4 of this report, results of scaling assessments of the important separate effects, integral effects, and containment tests are presented.

5.1.1 Separate Effects Tests

For the separate effects phenomena, it was shown that the AP600 Core Makeup Tank Test, the ADS tests, and the PRHR tests are sufficient to support licensing the AP1000. These separate effects tests sufficiently bound the expected AP1000 operating conditions.

5.1.2 Integral Effects Tests

The small-break LOCA transients are the most challenging for passive plants as nearly all of the passive safety features are employed to mitigate the transient and the transient includes broad ranges of thermal-hydraulic behavior. Therefore, three scaled integral effects test facilities were employed in the AP600 test program to provide data for computer code validation. Detailed scaling studies of two integral effect tests (SPES-2 and OSU) are presented in this report. Top-down scaling is particularly useful for evaluating the acceptability of an existing AP600 test program to a new design such as AP1000. The overall conclusion of the scaling studies of integral effects tests are as follows:

1. SPES-2 is adequately scaled to AP600 and AP1000 during the high-pressure phases of the SBLOCA transient. This includes blowdown through ADS depressurization phases to the actuation of ADS-4. The oversized ADS-4 at SPES-2 distorts the facilities' use for ADS to IRWST transition and IRWST injection phases.

2. OSU is adequately scaled to AP600 and AP1000 during the low-pressure phases of the SBLOCA transient when pressure similitude exists. This includes the ADS to sump injection phases where pressure similitude is maintained in OSU, and therefore scaling distortions are small.

3. The blowdown phase of the small break LOCA is a well-tested phase that is not unique to passive plants. The phase ends in a quasi steady-state phase of natural circulation. During the Blowdown phase there is no challenge to core inventory or core cooling.

4. The top-down scaling of test facilities to the AP1000 is acceptable for SPES-2 for the Natural Circulation, ADS, ADS-IRWST transition phases of the small break LOCA transient. The top-down scaling of OSU is acceptable for the ADS-IRWST transition, IRWST injection and sump injection phases. All phases of the small break LOCA are acceptably scaled at one of the integral test facilities and the "transition phase" of ADS-IRWST transition is acceptably scaled at both facilities.

5. Bottom-up scaling is used to address important local effects that are identified as important in the PIRT. For the bottom-up analysis addressed in this report the scaling is acceptable for one of the two integral test facilities, with the exception of pressurizer drain in the ADS-IRWST transition phase, which is marginally scaled at OSU. For this phenomenon the test scaling to AP1000 is better than the test scaling to AP600.

6. The scaling results demonstrate the value of having multiple test facilities:

    - As distortions are inevitable in any test facility; it is valuable to have multiple facilities to cover all important phenomena.

    - Multiple facilities also supports "validation" among test facilities. That is phenomena can be compared at different scales.

- Inclusion of the ROSA and OSU tests sponsored by the NRC is expected to contribute additional certainty regarding scaling acceptability.

7. In most respects, AP600 and AP1000 are similarly scaled. The major difference is the AP1000 core power to RCS volume ratio is higher than AP600. This effects time during ADS phase transient.

8. Similar to the AP600, the AP1000 scaling assessments demonstrate that there is at least one integrals effects test facility sufficiently scaled to AP1000 to cover all important phenomena and phases.

To further illustrate that the two AP600 integral test facilities are properly scaled to AP1000, Tables 5-1 and 5-2 illustrate how the important phenomena are addressed in the scaling analyses for the various portions of the small break LOCA transient for the OSU and SPES-2 facilities respectively. Table 5-3 shows the comparison of AP600 to AP1000 with respect to SBLOCA scaling results. These tables illustrate that at least one of the integral effects test facilities is scaled sufficiently for the important phenomena identified for the small break LOCA transient. In addition, the separate effects tests supplement the integral effects tests for the ADS, CMT, and PRHR performance phenomena.

5.1.3 Containment Tests

With respect to the containment and the passive containment cooling system, the studies presented in Section 4 conclude the following:

1. Due to its relatively low and constant steam injection flow rate, the LST was not well scaled to model the blowdown transient condensation and convective energy transfer (π_{COND}, π_{CONV}) for either AP600 or AP1000. However, the steady state LST data was determined to be acceptable for use as a source of separate effects data for internal condensation, above-deck steam distribution, external heat transfer, and external water coverage for both the AP600 and AP1000.

2. The values for the AP600 and AP1000 dimensionless parameters used in scaling the heat and mass transfer correlations were compared to the values from the AP600 PCS test program. The AP600 PCS test program dimensionless parameter values for the selected heat and mass transfer correlations for condensation on the inside of the shell and evaporation/convection on the outside of the shell in the important riser region of the annulus covered both the AP600 and AP1000 operating range values.

3. Based on Fr number scaling of the break jet, the volume above the operating deck in both the AP600 and AP1000 is expected to be well mixed during the blowdown portion of a DBA event. Based on the HDR E11.4 test results, scalable separate effects test data and the CFD analysis results presented in this report, this volume above the operating deck is expected to be well mixed during the long-term heat removal phase of the DBA event, when condensation on the shell is occurring. Therefore, the use of a lumped

parameter node to model the volume above the operating deck is acceptable for both the AP600 and AP1000.

4. The operating ranges of the AP600 and AP1000 film coverage parameters were compared with the range of the PCS test data. The test data covered the operating range of the important film coverage parameters (minimum Re and maximum heat flux) for both AP600 and AP1000.

5.2 APPLICATION OF THE RESULTS OF AP1000 SCALING STUDIES

Based on the results presented in this report, Westinghouse concluded that the database of test information generated during the AP600 Design and Design Certification program is sufficient to meet the requirements of 10 CFR Part 52. Furthermore, the computer analysis codes validated using this test data should be applicable for the AP1000.

Based on the findings presented in this report, the following conclusions regarding thermal-hydraulic computer code validation can be drawn:

- For large break LOCA events, both the AP600 and the AP1000 behave like existing Pressurized Water Reactors. Analysis codes that acceptably predict AP600 and existing PWR performance will acceptably predict AP1000 performance.

- For small break LOCA events, computer codes that acceptably predict SPES-2 and OSU behavior can be used to conservatively analyze the performance of the AP1000. Moreover, codes that predict the high pressure phases of the transient (i.e., prior to ADS-4 actuation) will acceptably predict the high pressure portion of the SBLOCA transient for the AP1000 plant. Codes that predict the lower pressure phases (i.e., post ADS-4) will acceptably predict the performance of the AP1000 for the low pressure phases of the SBLOCA transient.

- Non-LOCA transients for passive plants are similar to existing PWRs with the addition of the PRHR heat exchanger and the core make up tank injection models. The PIRT and scaling of these two effects indicate that analysis codes that acceptably predict AP600 performance will acceptably predict AP1000 performance.

- Containment transients for the AP1000 and the AP600 are similar. An independent analysis of mixing above the operating deck predicts mixing in the AP1000 is the same as AP600. Analysis codes that acceptably predict AP600 containment performance will also acceptably predict AP1000 containment performance.

Reference 1 provided results of safety analysis evaluations of the AP1000 using the AP600 computer codes to show the expected operating range of the AP1000 passive safety systems. These analyses indicated that the AP600 and AP1000 operated in a similar range of conditions for those events analyzed. A specific code applicability report for the computer codes that Westinghouse plans to use in support of Design Certification for the AP1000 will be presented in a separate report.

5.3 REFERENCE

1. WCAP-15612, "AP1000 Plant Description and Analysis Report," M. M. Corletti et al., December 2000.

Table 5-1A Summary of SBLOCA Top-Down Scaling Results – OSU Test Facility

a,b,c

Table 5-1A (cont.) Summary of SBLOCA Top-Down Scaling Results – OSU Test Facility

a,b,c

Table 5-1B Summary of SBLOCA Bottom-Up Scaling Results – OSU Test Facility

a,b,c

Table 5-2A Summary of SBLOCA Top-Down Scaling Results – SPES Test Facility

a,b,c

Table 5-2A (cont.) Summary of SBLOCA Top-Down Scaling Results – SPES Test Facility

a,b,c

Table 5-2B Summary of SBLOCA Bottom-Up Scaling Results – SPES Test Facility

a,b,c

Table 5-3A Summary of SBLOCA Top-Down Scaling Results – Comparison of AP600 to AP1000

a,b,c

Table 5-3A (cont.) Summary of SBLOCA Top-Down Scaling Results – Comparison of AP600 to AP1000

a,b,c

Table 5-3B Summary of SBLOCA Bottom-Up Scaling Results – Comparison of AP600 to AP1000

a,b,c

APPENDIX A
AP600 PROGRAM TEST SUMMARIES

The following provides a summary of each AP600 test including their purpose, a description of the facility, a discussion of the test matrix/results. The use of these tests in the AP1000 program are discussed in Section 3.0.

A.1 PASSIVE CORE COOLING SYSTEM (PXS) TEST SUMMARIES

The following tests were performed for the PXS.

- Departure from Nucleate Boiling (DNB) test (subsection A.1.1)
- Passive Residual Heat Removal Heat Exchanger (PRHR HX) test (subsection A.1.2)
- Automatic Depressurization System (ADS) test , phase A (subsection A.1.3)
- ADS test, phase B (subsection A.1.4)
- Core Makeup Test (CMT) test (subsection A.1.5)
- Low-pressure, integral systems test, OSU (subsection A.1.6)
- Low-pressure, integral systems test, OSU-NRC (subsection A.1.7)
- High-pressure, integral systems test, SPES-2 (subsection A.1.8)
- High-pressure, integral systems test, ROSA-AP600 (subsection A.1.9)

A.1.1 DNB Tests

General Purpose/Description

While low-flow DNB tests have been performed successfully on other fuel assembly geometries, data accumulated over several years of testing on the current Westinghouse fuel designs have concentrated on the higher flow range associated with operating conditions of conventional, higher-power density cores. The purpose of these tests was to determine the critical heat flux (CHF) performance of the AP600 fuel assembly design, particularly at low-flow conditions. In addition, the effect on CHF of the intermediate flow mixer (IFM) grids at low-flow conditions was measured.

The test objective was to gather CHF data on typical and thimble cell AP600 bundle geometry covering the range of fluid conditions anticipated during AP600 DNB-related ANS Condition I and II transients. The conditions cover the following ranges:

Pressure:	1500 to 2400 psia
Mass velocity:	0.5 to 3.5 x 10^6 lbm/hr-ft^2
Inlet temperature:	380° to 620°F

Also, a typical cell test where the AP600 bundle has the IFM grids replaced by simple support grids (SSGs) was run to assess the effect of the IFMs at low-flow conditions.

To perform a series of low-flow tests, two test bundles were constructed. The test bundles consisted of a small 5 by 5 array of rods, which are electrically heated and well-instrumented with thermocouples. The components for the test bundles were shipped to the test site, Columbia University, and assembled just prior to testing.

Test Results/Matrix

Sufficient data were taken to provide a basis for reducing the lower limit on mass velocity by 60 to 70 percent from the current value of 0.9 by 10^6 lb/hr-ft^2 (i.e., to the 3 to 4 fps range).

The results of the DNB tests were used to extend the existing Westinghouse DNB correlation to lower flow rates than previously tested. Other correlations, however, did extend to lower flow rates, and the DNB margin has been shown to exist using these correlations over the lower range of flow rates. Since the AP600 has ample DNB margin, this test did not impact the core or fuel design.

A.1.2 PRHR HX Test

General Description/Purpose

An experimental program was performed to characterize the thermal performance of the PRHR HX and the mixing behavior of the in-containment refueling water storage tank (IRWST). The experiment used stainless steel tubing material, tube diameter, pitch and length. The tubes were located inside a scaled IRWST. Since the vertical length was preserved, the buoyant-induced flow patterns inside the tank simulated the AP600. The main scaling parameter for the experiment was the pool volume per HX tube so that the heat load characteristics, resulting tank fluid conditions, and induced flow pattern would be similar to those in the AP600.

Test Matrix/Results

The PRHR HX test confirmed the heat transfer characteristics of the PRHR HX and mixing characteristics of the IRWST. These results validated the HX size and configuration.

The test conditions covered a full range of expected flow rates, including forced-convection PRHR cooling [reactor coolant pumps (RCPs) running] and natural circulation flows by varying the pumped flow through the tubes. The tests also examined different initial primary fluid temperatures over a range from 250° to 650°F using hot pressurized water that flowed downward inside the tubes. The initial tank temperature was either ambient temperature (70°F) or near boiling (212°F). The test data were reduced to obtain the local wall heat flux on the PRHR tubes. Comparisons of the PRHR test data with existing correlations for free convection and boiling were made, and a design correlation for the PRHR HX was developed.

The following conclusions were drawn from the test results:

- A boiling heat flux correlation similar to recognized correlations was developed from the PRHR data. Using the PRHR boiling correlation, an overall heat transfer coefficient can be calculated to determine the required surface area and evaluate the PRHR performance during postulated accidents.

- Mixing of the water in the simulated IRWST was very good. Localized boiling did not occur until the entire IRWST water volume was significantly heated. The test demonstrated that the IRWST water will not steam into the AP600 containment for about 2 hours.

A.1.3 ADS Test - Phase A

General Description/Purpose

The purpose of these tests was to simulate operation of the ADS, to confirm the capacity of the ADS, and to determine the dynamic effects on the IRWST structure.

The ADS phase A test was a full-sized simulation of one of the two AP600 depressurization system flow paths from the pressurizer that duplicated or conservatively bounded the operating conditions of the AP600 ADS valves, sparger, and IRWST. A full-sized sparger was tested. The loadings on the sparger and its support were measured, as were temperatures and pressures throughout the test arrangement.

A pressurized, heated water/steam source was used to simulate the water/steam flow from the AP600 RCS during ADS operation. The flow was piped to a full-sized sparger submerged in a circular rigid quench tank simulating the IRWST. Instrumentation to measure water and steam flow rate, equipment dynamic loads, IRWST dynamic loads, and sparger/IRWST steam quenching was provided.

The ADS phase A test arrangement is shown schematically in Figure A.1-1 Phase A testing consisted of saturated steam blowdowns, at rates simulating ADS operation, through the submerged sparger. Sparger steam quenching was demonstrated from ambient to fully saturated IRWST water temperatures.

Test Matrix/Results

Phase A was conducted to provide both the maximum possible blowdown rate when all three stages of the AP600 ADS were actuated, and to simulate the minimum blowdown rate (end of blowdown) when the pressurizer was essentially depressurized. For these tests, all three piping connections between the test drum and the discharge line were open. These tests were used to select the quench tank water level to be used in all subsequent ADS blowdowns.

Tests were performed to simulate the actuation of the first stage of ADS and blowdown to 500 psig. One test simulated the inadvertent opening of a second- or third-stage ADS valve when the reactor is at operating pressure. Additional tests provided the maximum blowdown rate that will occur in the AP600 when the first- and second-stage ADS valves are open.

Results of the phase A tests were used to verify the design of the ADS sparger and obtain sufficient information to perform preliminary design of the IRWST. Tests performed with a fully saturated quench tank water showed that loads on the IRWST decrease as water temperature increases.

A.1.4 ADS Test - Phase B

General Description/Purpose

The ADS phase B test was a full-sized simulation of one of the two AP600 depressurization system flow paths from the pressurizer that duplicated the operating conditions of the AP600 ADS valves, sparger, and IRWST. A full-sized ADS valve piping package was tested. The loadings on the sparger and its support were measured, as were temperatures and pressures throughout the test arrangement.

Phase B testing was performed at ENEA's VAPORE test facility in Casaccia, Italy. The test collected sufficient thermal-hydraulic performance data to support the development and verification of analytical models of the ADS used in safety analyses of events for which the ADS is actuated. In addition, it provided the design requirements of the ADS components and obtained sufficient information to establish component design specifications.

Phase B testing included the addition of piping to permit the blowdown of either saturated steam or saturated water from the pressurizer, and installation of piping and valves representative of the actual ADS. The ADS phase B test arrangement is shown schematically in Figure A.1-2. Figure A.1-3 shows the prototypic sparger being installed in the facility quench tank.

ADS phase B test data were used to assess the critical and subsonic flow models for the valves in the ADS system, as well as the sparger, when the flow is two-phase. ADS phase B tests supported proper specification of the functional requirements for the valves.

Test Matrix/Results

The test matrix is shown in Table A.1-1. Tests were run with various ADS valve flow areas. The final test report has been written. The key results and observations for ADS phase B are:

- The sparger operated properly over the full range of ADS flow rates, fluid qualities, and quench tank temperatures.
- ADS quench tank loads resulting from sparger-induced pressure pulses during phase A are conservative.
- Loads observed for steam and steam/water blowdowns are less than phase A.
- Data for water through the piping and valves were obtained and appear to be similar to the AP600.
- No low-flow slugging was exhibited by the sparger.
- Blowdowns into a hot (212°F) quench tank produced small loads.

A.1.5 CMT Test

General Description/Purpose

The purpose of this test was:

- to simulate CMT operation over a wide range of prototypic pressures and temperatures
- to simulate CMT operability
- to simulate the operability of the CMT level instrumentation
- to obtain data to support the development and verification of computer models to be used in safety analyses and licensing of the AP600 design.

The CMT test facility consisted of a CMT tank, a steam/water reservoir, instrumentation, and associated steam supply inlet and water discharge piping and valves (Figure A.1-4). A layout comparison between the AP600 CMT and RCS, and the CMT test tank and steam/water reservoir is provided in Figure A.1-5. The CMT used in the test was a carbon steel pressure vessel about 2 ft in diameter and 10 ft in overall length. The tank was mounted vertically and elevated so that the height between the bottom of the tank and the steam/water reservoir was equivalent to the initial head for gravity draining available in the plant. The CMT steam supply line from the steam water reservoir to the CMT simulated the cold leg to the CMT balance line. During testing, only one of the two steam lines were open. Steam line 1 had higher resistance than steam line 2 and connected to the top of the steam/water reservoir. Steam line 2 projected into the steam water reservoir and was heat-traced to better simulate the cold-leg balance line. The steam water reservoir was used to provide a source of steam to the CMT and to collect the water discharged from the CMT. Thus, it acted as a simulated RCS for the test facility.

The CMT test was designed to accommodate a device used to reduce steam jetting directly into the tank. A steam distributor (consisting of a short pipe with a series of holes in the cylindrical section of the pipe and a capped end, attached to a flange) was inserted into the inlet piping to test the effectiveness of the device during the hot pre-operational tests.

The performance of an instrument that may have the characteristics for the desired plant level instrumentation was obtained for this CMT test program. To test the operation and performance of the CMT level instrumentation which may be used in the actual plant, four pairs of resistance temperature detectors, each pair consisting of one heated resistance temperature detector and one unheated, were located at different elevations on their test tank. The output signals from the four resistance temperature detector pairs were recorded during each matrix test. The data was analyzed by the instrumentation engineers and the performance of the instrument characterized and evaluated at the conclusion of the test program to determine their overall performance and establish design criteria and specifications for the actual plant level instrumentation. The CMT test level measurement system data will be analyzed to assess the behavior of the CMT differential pressure cells and the response of the CMT level device to a wide range of thermodynamic conditions.

Technical justification that the data from the CMT test size and configuration in this and the SPES-2 and OSU tests can be extrapolated to the plant CMT conditions via analysis, particularly with regards to two- and three-dimensional effects, is provided in the CMT scaling report. These tests capture the thermal-hydraulic phenomena that a full-sized CMT would display.

Test Matrix/Results

Shakedown testing was used to establish system volumes, line resistances, valve positions required to establish specific steam injection, and CMT draindown rates. The matrix tests are provided in Table A.1-2.

The objectives of the CMT matrix tests were:

- To simulate CMT conditions and measure the rate of steam condensation on the CMT walls and water surface versus steam pressure and water-drain rate
- To obtain detailed measurements of CMT through-wall temperature profiles, CMT liquid inventory temperature profiles, and condensate drain rates versus steam pressure
- To simulate stable behavior of the CMT water level as the cold water drains and is replaced by steam over a wide range of drain rates and piping resistances bounding the prototypic design
- To evaluate the operation of CMT level instrumentation used to actuate the ADS at typical CMT conditions

During CMT hot pre-operational testing, the model CMT diffuser was plastically deformed. Through examination and analysis of this CMT diffuser, Westinghouse determined the root cause. During preoperational testing of high-pressure steam injecting into an empty tank, the diffusers were subjected to a high differential pressure in conjection with high temperatures, beyond the system design basis. The diffuser suffered fatigue failure, which is not expected within an AP600 plant operating life. Other diffusers used during more prototypic tests performed without incident.

The key results and observations are:

- The test tank operated over the full range of pressures, temperatures, and flow rates.
- Sufficient data were obtained for model development and code validation for recirculation and draindown.
- The steam diffuser reduced condensation and limited mixing to about 12 inches below the diffuser, without waterhammer.
- Hydraulics of the test were well predicted by using simple mass and energy equations.

- Narrow range differential pressure level sensors were selected for use in the AP600 based on their ability to accurately measure water levels in the tests.

A.1.6 Low-Pressure Integral Systems Test (OSU)

General Description/Purpose

The low-pressure, 1/4-height integral systems test was conducted at the Corvalis campus of OSU. Scaling studies indicated that a scaled low-pressure test facility could capture the thermal-hydraulic phenomena of interest for the lower pressure behavior of the AP600.

The OSU test facility is a new facility constructed specifically to investigate the AP600 passive system behavior. The test design accurately modeled the detail of the AP600 geometry including the primary system, pipe routings, and layout for the passive safety systems. The primary system consisted of one hot leg and two cold legs with two active pumps and an active steam generator (SG) for each loop, shown in Figure A.1-6. There were two CMTs connected to one primary loop; the pressurizer was connected to the other primary loop, as in the AP600 plant design. Gas-driven accumulators were connected to the direct vessel injection (DVI) lines. The discharge lines from the CMT and one-of-two IRWST and reactor sump lines were connected to each DVI line. The two independent tiers of ADS-1/2/3 valves were lumped together as a single ADS stage. The two-phase flow from the ADS stages one, two, and three were separated in a swirl-vane separator. The liquid and vapor flows were measured to obtain the total ADS flow rate. The separated flow streams were then recombined and discharged into the IRWST through a sparger. Thus, the mass flow and energy flow from the ADS into the IRWST were preserved.

The time period for the simulation included not only IRWST injection, but long-term containment recirculation operation of the AP600. The duration of this simulation was from several hours to a half day. The time scale for the OSU test facility was about one-half, i.e., phenomena occur at twice the rate of OSU as in the AP600.

To model the long-term cooling aspects of the transient, two-phase flow from the break was separated in a swirl-vane separator, and the liquid and vapor portions of the total flow were measured. The liquid fraction of the flow was discharged to the reactor sump, as in the AP600 plant; the vapor was discharged to the atmosphere; and the equivalent liquid flow was added to the IRWST and reactor sump to simulate condensate return from passive containment. A similar approach was used for the fourth-stage ADS valve on the hot leg. Two-phase flow was separated in a swirl-vane separator; the two streams were measured; the liquid phase was discharged into the reactor sump, the vapor flow was discharged to the atmosphere, and the liquid equivalent was added to the IRWST and LCS. The IRWST and LCS can be pressurized to simulate containment pressurization following a postulated LOCA.

A multi-tube PRHR HX is located in the IRWST. The HX uses the same C-tube design as the AP600 and has two instrumented tubes to obtain wall heat fluxes during tests. There are primary fluid thermocouples, wall thermocouples, and differential pressure drop measurements to determine when the HX begins to drain. The IRWST is also instrumented with strings of fluid thermocouples to determine the degree of mixing in the tank and assess the temperature of the coolant delivered to the test vessel.

The reactor vessel for the OSU tests included a 3-ft heated core simulator consisting of 48 1-inch diameter heater rods. The heater rods had a top-skewed power shape. There were wall thermocouples swaged inside the heater rods to measure the heater rod wall temperature. There were also five thermocouple rods in the heater rod bundle, including fluid thermocouples, to measure the axial coolant temperature distribution. The scaled flow area in the core and flow area in the test vessel upper plenum were preserved. There were simulated reactor internals in the upper plenum to preserve the flow area and the correctly scaled fluid volume. The reactor vessel included an annular downcomer into which the four cold legs and the DVI lines were connected. The hot legs penetrated the reactor annulus and connected with the loops. The AP600 reactor vessel neutron reflector was simulated using a ceramic liner to reduce the metal heat release to the coolant.

There was about 1.5 E09 J/hr (640 kW) of electrical power available at the OSU test site, which corresponds to a decay heat of 2 percent of full power in the AP600.

Test Matrix/Results

The OSU experiments examined the passive safety system response for the SBLOCA transition into long-term cooling. A range of small break loss-of-coolant accidents (SBLOCAs) was simulated at different locations on the primary system, such as the cold leg, hot leg, CMT cold-leg pressure balance line, and DVI line. The break orientation (top or bottom of the cold leg) was also studied. Different single failure cases were examined to confirm that the worst situation was used in the AP600 Standard Safety Analysis Report (SSAR) analysis. Selected tests continued into the long-term cooling, post-accident mode in which passive SI was from the reactor sump as well as the IRWST. A larger-break, post-accident, long-term cooling situation was also simulated. A summary of the test matrix is provided in Table A.1-3.

A specific test was performed at the OSU test facility to examine the effects of a higher backpressure on an SBLOCA transient. A sensitivity study was also performed on the effects of containment backpressure, verifying the test assumptions.

The OSU test data was analyzed to determine the long-term cooling behavior of the system. The calculated mass and energy balances from the OSU test facility will be used to determine these effects. If needed, a simple transport model, using the OSU mass balance data as a method of verification, will be written to track the boron distribution.

The key results and observations for the OSU test are:

- The core remained covered for all design basis transients although there were oscillations during long-term recirculation operations.

- All passive systems functioned as expected, with no adverse consequences, including CMT recirculation and draindown, PRHR HX heat removal, ADS depressurization, accumulator injection, IRWST gravity draining, and stable long-term sump injection.

- The CMTs refilled due to condensation effects during long-term recirculation.

- Minor steam condensation events occurred in the upper downcomer region.

- Thermal stratification occurred in both the hot and cold legs.

A.1.7 Low Pressure, Integral Systems Test (OSU-NRC)

The NRC conducted additional testing at the OSU test facility. Some small changes were made to the facility with respect to the ADS-1/2/3 flow capacity to improve scaling at low pressure and some instrumentation was improved. The objective of the tests were to provide the NRC confirmatory data in support of licensing the AP600. Tests performed included multiple failure scenarios that would severely challenge the passive safety systems capabilities and demonstrated the robustness in the AP600 design. Table A.1-4 provides the OSU-NRC test matrix. Westinghouse did not use this test data in its AP600 design or licensing activities.

A.1.8 High-Pressure, Integral Systems Test (SPES-2)

General Description/Purpose

A full-pressure, full-height integral systems test was performed to provide a simulation of the passive core cooling system (PXS) system integrated performance. The existing SPES test facility was configured as a full-height, full-pressure integral test with AP600 features, including two loops with one hot leg and two cold legs per loop, two CMTs, two accumulators, a PRHR HX, an IRWST, and an ADS. The facility included a scaled reactor vessel, SGs, pressurizer, and RCPs. Water was the working fluid, and core power was simulated with electric heater rods.

The test facility was designed to be capable of performing tests representative of a SBLOCA, steam generator tube rupture (SGTR), and steam line break (SLB) transients. The design certification analysis was compared to the test results.

The facility simulated the following:

- Primary circuit

- Secondary circuit up to the main steam line isolation valve

- All passive safety systems — CMT, IRWST, PRHR HX, ADS

- Nonsafety NSSS systems — chemical and volume control system (CVS), normal residual heat removal system (RNS), and startup feedwater system (SFWS)

A scaling, design, and verification analysis has been made to delineate the specific design features to be incorporated and modifications to be made to the SPES-1 facility to simulate the AP600 design.

The following general criteria have been applied to the design of the SPES-2 test facility:

- Conservation of thermodynamic conditions (pressure and temperature)
- Power over volume ratio conservation in each component
- Power over mass flow rate conservation
- Fluid transit time preservation
- Heat flux conservation in heat transfer components (core and SG)
- Elevations maintained in lines and components
- Preservation of Froude number in the primary circuit loop piping (hot and cold legs) in order to preserve the slug to stratified flow pattern transition in horizontal piping

The SPES-2 facility consisted of a full simulation of the AP600 primary and passive core cooling systems. The stainless steel test facility used a 97-rod heated rod bundle with a uniform axial power shape and skin heating of the heater rods. The tests were initiated from scaled, full power conditions. There were 59 heater rod thermocouples distributed over 10 elevations with most located at the top of the bundle to detect the possibility of bundle uncovery. The heater rods were single-ended, connected to a ground bus at the top of the bundle at the upper core plate elevation. All but two rods were designed to have the same power; two heater rods were "hot" rods that had 19 percent higher power.

The primary system, shown in Figure A.1-7, included two loops each with two cold legs, one hot leg, an SG, and a single RCP. The cold leg for each loop was divided downstream of the simulated RCP into two separate cold legs, each of which connected into an annular downcomer. The pumps delivered the scaled primary flow, and the heater rod bundle produced the scaled full-power level so that the AP600 steady-state temperature distribution was simulated. The SGs had a secondary side cooling system that removed heat from the primary loop during simulated full-power operation. Startup feedwater and power-operated relief valve heat removal was provided following a simulated plant trip.

The upper portion of the simulated reactor vessel included an annular downcomer region, where the hot and cold legs as well as the SI lines were connected as shown in Figure A.1-8. The annular downcomer was connected to a pipe downcomer below the DVI lines; the pipe downcomer then connected to the vessel lower plenum. In this fashion, the four cold-leg/two hot-leg characteristics of AP600 were preserved, along with the downcomer injection. There were turning devices to direct the safety injection (SI) flow down in the annular downcomer as in the AP600.

A full-height single PRHR HX, constructed in a C-tube design, was located in a simulated IRWST and maintained at atmospheric pressure. The line pressure drop and elevations were preserved, and the heat transfer area was scaled so that the natural circulation behavior of the AP600 PRHR HX was simulated.

The design of the CMTs was developed so that the CMT metal mass was scaled to the AP600 CMT. The CMT design used a thin-walled vessel inside a thicker pressure vessel, with the space between the two vessels pressurized to about 70 bar. In this manner, the amount of steam that condensed on the CMT walls during draindown was preserved. Since the CMTs were full-height and operated at full pressure, the metal mass-to-volume of a single pressure vessel would have been excessive, resulting in very large wall steam condensation effects.

The SPES-2 ADS combined the two sets of AP600 ADS piping off the pressurizer into a single set with the first-, second-, and third-stage valves. An orifice in series with each ADS isolation valve was used to achieve the proper scaled flow area. The three ADS valves shared a common discharge line to a condenser and a collection tank that used load cells to measure the mass accumulation. A similar measuring arrangement was also used for the two ADS fourth-stage lines, which were located on the hot legs of the primary system. The SPES-2 tests simulated the AP600 transients up to the time of IRWST injection at low pressure.

Small breaks were simulated using a spool piece that contained a break orifice and quick-opening valve. The break discharge was also condensed and measured by collecting the flow into a catch-tank.

The SPES-2 facility instrumentation was developed to provide transient mass balances on the test facility. There were about 500 channels of instrumentation that monitored the facility, component pressure, temperature, density, and mass inventory. Flows into the simulated reactor system, such as CMT discharge flow, accumulator flow, and IRWST flow, were measured using venturi flow meters. Flows out of the test facility, such as break flow and ADS flow, were measured with a turbine meter and condenser/collection tank. The use of condensers allowed accurate integrated mass versus time measurements of the two-phase ADS and break-flow streams. The use of collection tanks following the condensers provided redundancy for the critical measurements of the mass leaving the test system. Differential pressure measurements were arranged as level measurements on all vertical components to measure the rate of mass change in the component. There were also differential pressure measurements between components to measure the frictional pressure drop, both for single- and two-phase flow. The CMTs were instrumented with wall and fluid thermocouples to measure the CMT condensation and heat-up during their operation. The PRHR HX was also instrumented with wall and fluid thermocouples so that the tube wall heat flux could be calculated from the data. There were thermocouples in the simulated IRWST to measure the fluid temperature distribution and assess the amount of mixing that occurred. Rod bundle power was measured accurately to obtain rod heat flux and total power input to the test facility.

Test Matrix/Results

The overall objectives of the AP600 SPES-2 integral system test were:

- To simulate the AP600 thermal-hydraulic phenomena and behavior of the passive safety systems following specified SBLOCAs, steam generator tube rupture (SGTRs), and SLBs.
- To obtain detailed experimental results for verification of safety analysis computer codes.

The SPES-2 test matrix (Table A.1-5) examined the AP600 passive safety system response for a range of SBLOCAs at different locations on the primary system, SGTRs with passive and active safety systems, and a main steam line break (MSLB) transient. The SPES-2 final test report was issued in April 1995.

Key results and observations for the SPES-2 test are:

- The core remained covered following all simulated events, included a DEG DVI line break with only passive safety systems operating.
- There was no CMT draindown; therefore, no ADS actuation occurred following the single SGTR with no operator action or nonsafety systems operating.
- Nonsafety system operation had no adverse interaction with passive system operation, and actually added margin to the plant safety response.
- All passive safety systems functioned as expected with no adverse occurrences including CMT recirculation and draindown, PRHR HX heat removal, ADS depressurization, and IRWST gravity draining.
- Timely RNS operation following a LOCA can limit CMT draindown and prevent ADS fourth-stage actuation.

A.1.9 High-Pressure, Integral Systems Test (ROSA-AP600)

A full-pressure, full-height integral systems test was performed to provide a simulation of the PXS system integrated performance. The existing ROSA test facility was modified to simulate an AP600, providing two loops including the reactor vessel, SGs, RCPs and pressurizer. The passive safety features connected to the RCS were simulated. Nonsafety systems providing makeup to the reactor and the SGs were also simulated. Water was the working fluid and the core was simulated with electrical heater rods. ROSA is a large scale facility, with about 1/30 of the AP600 primary side volume.

The test facility was designed to be capable of performing tests representative of a SBLOCA, SGTR, and SLB transients. The design certification analysis was compared to the test results.

The facility simulated the following:

- Primary circuit with one hot leg, cold leg, SG, RCP per loop and a pressurizer
- Secondary circuit up to the main steam line isolation valve
- Passive safety systems connected to the RCS – CMTs, accumulators, IRWST, PRHR HX and ADS
- Nonsafety NSSS systems - chemical and volume control system (CVS), normal residual heat removal system (RNS), and startup feedwater system (SFWS)

The ROSA/AP600 facility consisted of a full simulation of the AP600 primary and passive core cooling systems. The stainless steel test facility used a heated rod bundle with an axial power shape similar to the AP600 shape. The heater rod bundle was capable of producing about 16.5 percent of the scaled AP600 power. The tests were initiated from scaled, full power conditions.

The primary system, shown in Figure A.1-9, included two loops each with one cold leg, one hot leg, an SG, and a single RCP. Figure A.1-10 (sheets 1 and 2) show the elevations of the ROSA/AP600 facility. The RCPs have a shallow loop seal with a bypass to further reduce the influence of the loop seals. The cold legs and hot legs connect to the reactor vessel (RV) at the same elevation instead of the cold leg being slightly higher as in the AP600. Studies indicate that the facility adequately simulates the AP600.

A new pressurizer was added to ROSA/AP600 and was scaled to represent the AP600 pressurizer. The internal height of the pressurizer was preserved, and the internal flow area was scaled. Flow velocities within the pressurizer are therefore equivalent; hence, entrainment/de-entrainment phenomena are preserved. The pressurizer surge line was scaled to represent the AP600 surge line resistance and to represent the flooding of the line as closely as possible. The geometry of the connection to the hot leg, however, is not similar to the AP600. In the AP600, the surge line connects to the top of an inclined pipe, while the ROSA/AP600 surge line connects to the top of a horizontal pipe.

The AP600 passive safety features connected to the RCS were simulated in ROSA/AP600. Typically, the components were designed to preserve the volume scaling ratio of 1:30, to preserve the AP600 elevations, and to maintain similar hydraulic resistance in pipes.

A full-height single PRHR HX, constructed in a C-tube design, was located in a simulated IRWST and maintained at atmospheric pressure. The tube bundle was full-height; each tube was full diameter. The number of tubes was reduced to scale the heat transfer area. The line pressure drop and elevations were preserved so that the natural circulation behavior of the AP600 PRHR HX was simulated.

The internal volume of the CMTs has been scaled 1:30, and the internal height was preserved. As a result the tank shapes were not preserved, with the AP600 CMTs being nearly spherical, while the Large-Scale Test Facility (LSTF) CMTs are more cylindrical. The ROSA/AP600 CMTs each have a sparger at the top of the tank, which disperses flow from the balance line, like the AP600 CMTs. Insulation was added to the CMTs to reduce the scaling distortion caused by excessive heat loss.

Because ROSA/AP600 only has one cold leg per loop, the CMTs balance lines are normally connected to the same cold leg. This arrangement is referred to as the "common mode." Asymmetrical CMT behavior is limited with this arrangement however, so another configuration is provided that allows the balance lines to be connected to separate cold legs. This arrangement is referred to as the "separate mode." In this mode, the balance lines for one CMT is connected to the cold leg in the other loop.

The ROSA/AP600 ADS combined the two sets of AP600 ADS piping off the pressurizer into a single set with the first-, second-, and third-stage valves. An orifice in series with each ADS isolation valve was used to achieve the proper scaled flow area. The three ADS valves shared a common discharge line to an IRWST as in the AP600. The AP600 stage 4 of the ADS has 4 valves, two per hot leg. ROSA/AP600 simulated this arrangement with one ADS-4 valve per hot leg. An orifice in series with these ADS-4 valves allowed simulation of one or two ADS-4 valves opening for each hot leg. The ADS-4 lines are routed to catch tanks that are vented to the atmosphere.

The IRWST volume is about 34 percent underscaled. This is the result of design changes to the AP600 that occurred just after the IRWST had been installed. Consequently, because there is less liquid mass in the ROSA/AP600 IRWST, the liquid temperature will increase faster than that of the AP600 as the PRHR heat exchanger and the discharge from ADS-1/2/3 transfers energy to the liquid. The decrease in the static head that results from the discharge of a unit of liquid mass from the tank also became somewhat larger than the ideal. One test was conducted to evaluate the effect of the undersizing of the IRWST.

Small breaks were simulated using a spool piece that contained a break orifice and quick-opening valve. The break discharge was also condensed and measured by collecting the flow into a break flow storage tank. It is possible to condense break flow from two break locations, consequently double ended breaks can be simulated.

Prior to the ROSA/AP600 program, the facility already had in place the hardware needed to measure and control processes throughout the facility. Instrumentation was added to accommodate the passive safety features and other simulated systems of the AP600. Data from the instruments is recorded on magnetic disks in digital format. Process and instrumentation displays are located in the control room, as are alarms, actuators, controls, etc. Most of the facility functions that are required to conduct a test can be initiated from the control room.

Test Matrix/Results

The overall objective of the ROSA/AP600 integral system test was to provide data to allow the NRC to confirm the performance of the AP600 during small LOCAs, SGTRs, steam line breaks and station black outs.

The test matrix for the ROSA/AP600 testing is contained in Table A.1-6.

Table A.1-1 ADS Phase B Test Specification ADS Performance Test Matrix

Facility Configuration	Test Run No.	ADS Simulation	Supply Tank Pressure
Saturated water blowdowns from bottom of supply tank, no orifices in spool pieces, cold quench tank water	310	Stages 1, 2, and 3 open	High
"	311	Stages 1, 2, and 3 open	Intermediate
"	312	Stages 1, 2, and 3 open	Low
"	330	Stages 1 and 2 open	High
"	331	Stages 1 and 2 open	Intermediate
"	340	Stage 2 open (inadvertent opening)	High
Saturated water blowdowns from bottom of supply tank, orifices installed in spool pieces	250	Stage 2 open (inadvertent opening)	Intermediate
"	210	Stage 1 open	High
"	211	Stage 1 open	High
"	212	Stage 1 open	High
"	220	Stages 1 and 2 open	Intermediate
"	221	Stages 1 and 2 open	High
"	230	Stages 1 and 3 open	Intermediate
"	231	Stages 1 and 3 open	High
"	240	Stages 1, 2, and 3 open	Intermediate
Saturated water blowdowns from bottom of supply tank, orifices installed in spool pieces	241	Stages 1, 2, and 3 open	Low
"	242	Stages 1, 2, and 3 open	Low
Saturated steam blowdowns from top of supply tank, orifices installed in spool pieces	110	Stage 1 open	High
"	120	Stages 1 and 2 open	High
"	130	Stages 1 and 3 open	Intermediate
"	140	Stages 1, 2, and 3 open	High

Table A.1-1 ADS Phase B Test Specification ADS Performance Test Matrix (cont.)

Facility Configuration	Test Run No.	ADS Simulation	Supply Tank Pressure
Saturated water blowdowns from bottom of supply tank, no orifices in spool pieces, quench tank water at 212°F (100°C)	320	Stages 1, 2, and 3 open	High
"	321	Stages 1, 2, and 3 open	Intermediate
"	322	Stages 1, 2, and 3 open	Low
"	350	Stages 1 and 2 open	High
"	351	Stages 1 and 2 open	Intermediate

Table A.1-2 Matrix Tests, CMT Test

Test	Test Type	CMT Drain Rate	Steam Supply Pressure(s)	Comments
101	CMT wall condensation with and without noncondensable gases	CMT drain rate based on steam condensation rate and drain capability	10	CMT initially contains no water and is evacuated
102			135	
103			685	
104			1085	
105			2235	
106			10	CMT pressure with air (or N_2) to .236, 1.13, and 2.13 psia, respectively
107				
108				
301	CMT draindown at constant pressure	6	10	Low resistance steam supply line 2 utilized; drain rate controlled by discharge line resistance
302		6	135	
303		6	1085	
304		11	10	
305		11	135	
306		11	1085	
307		16	10	
308		16	135	
309		16	1085	
310		Max	10	
311		Max	135	
312		Max	1085	
317		6	45	
318		11	45	
319		16	45	
320		6	685	
321		11	685	
322		16	685	
323		Max	685	

Table A.1-2 Matrix Tests, CMT Test (cont.)

Test	Test Type	CMT Drain Rate	Steam Supply Pressure(s)	Comments
401	CMT draindown during depressurization	6/16 gpm	1085, depressurization to 20	Steam line 2 used
402				
403		Rate controlled by supply line 1 resistance	2235, depressurization to 20	Resistance set for 6/16 gpm drain rate
404				
501	Natural circulation followed by draindown and depressurization	Discharge line resistance set for 6/16 gpm drain rate	1085, depressurization to 20	Natural circulation until 1/5 of CMT heated
502				
503				Natural circulation until 1/2 of CMT heated
504				
505				Natural circulation until CMT fully heated
506				
507		Drain rate to be chosen based on results of tests 501-506	1835, depressurization to 20	1/5 CMT heated
508				1/2 CMT heated
509				CMT fully heated

Table A.1-3 Matrix Tests, Low-Pressure, 1/4-Height Integral Systems Test (OSU)

Test Category	Test Number	Description
Cold pre-operational tests	C01	CMT gravity drain
	C02	Accumulator tank drain
	C03	IRWST drain
	C04	CVS pump flow vs. pressure
	C05	RNS pump flow vs. pressure
	C06	SG feed flow vs. pressure
	C07	ADS 1-3 line flow test
	C08	ADS-4 line flow test
	C09	RNS injection flow test
	OSU-F-02	Reactor coolant forced circulation loop flow test
Hot pre-operational tests	HS01	Reactor power calorimetric
		Ambient heat loss determination
		PRHR loss determination
		SG performance test
		RCS heatup/cooldown test
	HS02	600-kW power level testing
		Reactor coolant natural circulation loop flow test
	HS03	Verify post-accident decay power
		Verify performance of ADS 2, 3, and 4
		Determine performance of IRWST and sump injection

Table A.1-3 Matrix Tests, Low-Pressure, 1/4-Height Integral Systems Test (OSU) (cont.)	
Test Number	**Description**
SB01 •	2-inch cold-leg break, bottom of pipe, loop A with continuation into long-term cooling mode, fail one in ADS-4 stage
SB02	2-inch cold-leg break, bottom of pipe, loop A, fail one in ADS-4 stage
SB03	2-inch cold-leg break, bottom of pipe, loop A, fail one in ADS-4 stage
SB04	2-inch cold-leg break, bottom of pipe, loop A with nonsafety systems on, fail one in ADS-4 stage
SB05	1-inch cold-leg break, bottom of pipe, loop A, with continuation into LTC, fail one in ADS-4 stage
SB06	4-inch cold-leg break, bottom of pipe, loop A, fail one in ADS-4 stage
SB07	2-inch cold-leg small break, bottom of pipe, loop A, fail train of ADS 4-1
SB09	2-inch break on cold-leg balance line, horizontal loop, loop A, fail one in ADS-4 stage
SB10	DEG break of cold-leg balance line, horizontal loop, loop A with continuation into LTC, fail one in ADS-4 stage
SB11	DEG break of DVI line with continuation into LTC, fail one in ADS-4 stage
SB12	DEG break of DVI line, continuation into LTC, loss of one train of ADS-1 and ADS-3
SB13	2-inch break of DVI line, continuation into LTC, fail one in ADS-4 stage
SB14	Inadvertent ADS stage 1 open, with continuation into LTC, fail one in ADS-4 stage
SB15	2-inch hot-leg break, bottom of pipe, loop A, fail one in ADS-4 stage
SB18	2-inch cold-leg break, loop A, fail one in ADS-4 stage
SB19	SB01 with simulated containment backpressure, fail one in ADS-4 stage
SB21	Simulated long-term cooling, fail one in ADS-4 stage
SB23	1/2-inch cold leg break, bottom of pipe, loop A, fail one in ADS-4 stage
SB24	1/2-inch cold leg break, bottom of pipe, loop A, with nonsafety systems on, fail one in ADS-4 stage
SB25	Mid-loop operation test

Table A.1-3 Matrix Tests, Low-Pressure, 1/4-Height Integral Systems Test (OSU) (cont.)

Test Number	Description
SB26	PRA multiple failures without PRHR
SB27	Inadvertent ADS-1, fail one in ADS-4 stage
SB28	PRA case DEG DVI line break
SB29	2-inch cold leg break, bottom of pipe, loop A, fail one in ADS-4 stage
SB31	Spurious S signal without ADS, fail one in ADS-4 stage

Table A.1-4 Matrix Tests, Low-Pressure Integral Systems Test, OSU-NRC

Test #	ID #	Simulation	Break (in.)	Loc.	ADS-1 (%)	ADS-2 (%)	ADS-3 (%)	ADS 4-1 (%)	ADS 4-2 (%)
NRC-1	5001	1" CL Break with Failure of ADS 1-3 (ROSA Counterpart)	0.1604	CL3	Failed Shut	Failed Shut	Failed Shut	100	100
NRC-2	5002	Station Blackout	None	NA	100*	100*	100*	50*	100*
NRC-2	5102	Station Blackout	None	NA	100*	100*	100*	50*	100*
NRC-3	5003	2" CL Break with Long Term Cooling	0.3208	CL3	100	100	100	50	100
NRC-4	5004	2" CL Break – Flow Oscillation Assessment	0.3208	CL3	100	100	100	50	100
NRC-5	5005	1/2" CL Break	0.053	CL3	100	100	100	50	100
NRC-5	5105	1/2" CL Break	0.053	CL4	100	100	100	50	100
NRC-6	5006	1" CL Break with Full Pressure ADS	0.1063	CL3	50	50	50	100	100
NRC-7	5007	1" CL Break without ACC Nitrogen Injection	0.1063	CL3	100	100	100	100	50
NRC-7	5107	1" CL Break without ACC Nitrogen Injection	0.1063	CL3	100	100	100	100	50
NRC-10	5010	1" CL Break with Failure of 3 of 4 ADS Valves	0.1063	CL3	100	100	100	100	Failed Shut
NRC-11	5011	2" CL Break with Revised ADS 1-3 Flow Area	0.3208	CL3	100	100	100	100	50
NRC-11	5111	2" CL Break with Revised 1-3 Flow Area	0.3208	CL3	100	100	100	100	50
NRC-12	5112	2" CL Break	0.3208	CL4	100	100	100	100	50
NRC-14	5014	1" CL Break with Full Pressure ADS and Failure of 1 of 4 ADS-4	0.1063	CL3	50	50	50	50	100
NRC-15	6015	1" CL Break with Full Pressure ADS and Revised ADS Flow Area	0.1063	CL3	50*	50*	50*	50*	100*
NRC-18	6018	2" CL Break with Reactor Pressure Vessel Bypass Holes Plugged	0.3208	CL3	100	100	100	100	50
NRC-19	6019	1" CL Break with Reactor Pressure Vessel Bypass Holes Plugged	0.1063	CL3	100	100	100	100	50
NRC-20	6020	DEDVI Line Break (W-SB-11 Counterpart)	DEDVI	DVI	100	100	100	50	100

Table A.1-4 Matrix Tests, Low-Pressure Integral Systems Test, OSU-NRC (cont.)

Test #	ID #	Simulation	Break (in.)	Loc.	ADS-1 (%)	ADS-2 (%)	ADS-3 (%)	ADS 4-1 (%)	ADS 4-2 (%)
NRC-21	6021	1″ CL Break (ROSA AP-CL-03 and W-SB-5 Counterpart)	0.1063	CL3	100	100	100	50	100
NRC-22	6022	1″ CL Break (ROSA AP-CL-03 and W-SB-5 Counterpart)	0.1063	CL3	100	100	100	50	100
NRC-23	6023	Inadvertent ADS with Hot CMTs	None	NA	100	100	100	100	100
NRC-24	6024	Inadvertent ADS with Cold CMTs	None	NA	100	100	100	100	100
NRC-26	7026	1″ CL Break with Delayed Core Heatup	0.1063	CL3	Failed Shut	Failed Shut	Failed Shut	100	100
NRC-27	7027	1″ Break with Degraded Sump	0.1063	CL3	100	100	100	100	50
NRC-28	7028	DEDVI with Failure of Intact CMT	DEDVI	DVI	Failed Shut	Failed Shut	Failed Shut	100	50
NRC-29	7029	DEDVI with Failure of Intact ACC	DEDVI	DVI	Failed Shut	Failed Shut	Failed Shut	100	50
NRC-31	7031	1″ CL Break with High Decay Power and Degraded Sump	0.1063	CL3	100	100	100	100	50
NRC-32	7032	1″ CL Break with Failure of PRHR (Top of Cold Leg)	0.1063	CL3	100	100	100	100	50
NRC-35	8035	Mode 5 Cold Shutdown with Loss of RNS Cooling	None	NA	Failed Shut	Failed Shut	100	100	50

*Based on nominal sizes for ROSA ADS

Table A.1-4 Matrix Tests, Low-Pressure Integral Systems Test, OSU-NRC (cont.)

Test #	ID #	Simulation	Break (in.)	Loc.	ADS-1 (%)	ADS-2 (%)	ADS-3 (%)	ADS 4-1 (%)	ADS 4-2 (%)
100NRC-13 Return to Saturation Oscillation Test Series									
NRC-13	5013	Oscillation Test	0.3208	CL3	Failed Shut	Failed Shut	Failed Shut	50	100
NRC-13	6113	Oscillation Test	0.3208	CL3	Failed Shut	Failed Shut	Failed Shut	50	100
NRC-13	6213	Oscillation Test	0.3208	CL3	Failed Shut	Failed Shut	Failed Shut	50	100
NRC-25 No Reserve Core Uncovering Test Series									
NRC-25	6025	100 psia ADS-4 Blowdown	None	NA	Failed Shut	Failed Shut	Failed Shut	50	Failed Shut
NRC-25	6125	100 psia ADS-4 Blowdown	None	NA	Failed Shut	Failed Shut	Failed Shut	50	Failed Shut
NRC-25	6225	200 psia ADS-4 Blowdown	None	NA	Failed Shut	Failed Shut	Failed Shut	50	Failed Shut
NRC-25	6325	200 psia ADS-4 Blowdown	None	NA	Failed Shut	Failed Shut	Failed Shut	50	Failed Shut
NRC-25	6425	100 psia ADS-4 Blowdown	None	NA	Failed Shut	Failed Shut	Failed Shut	Failed Shut	100
NRC-25	7525	200 psia ADS-4 Blowdown	None	NA	Failed Shut	Failed Shut	Failed Shut	50	Failed Shut
NRC-25	7625	100 psia ADS-4 Blowdown	None	NA	Failed Shut	Failed Shut	Failed Shut	100	Failed Shut
NRC-25	7725	100 psia ADS-4 Blowdown	None	NA	Failed Shut	Failed Shut	Failed Shut	100	Failed Shut
NRC-25	7825	100 psia ADS-4 Blowdown	None	NA	Failed Shut	Failed Shut	Failed Shut	Failed Shut	50
NRC-25	7925	100 psia ADS-4 Blowdown	None	NA	Failed Shut	Failed Shut	Failed Shut	Failed Shut	50
NRC-34 Nitrogen Transport Test Series									
NRC-34	7034	1″ CL Break with Argon-41 Tracer	0.1063	CL3	100	100	100	100	50
NRC-34	7134	1″ CL Break with Argon-41 Tracer	0.1063	CL3	100	100	100	100	50
NRC-34	7234	1″ CL Break with Argon-41 Tracer	0.1063	CL3	100	100	100	100	50

Table A.1-5 Matrix Tests, Full-Pressure, Full-Height Integral Systems Test (SPES-2)		
Test Category	**Test Number**	**Description**
Cold shakedown tests	C-01	Single-phase flow through the pressurizer surge line, four flow rates
	C-02A,B	Single-phase flow through the pressurizer to CMT balance lines, four flow rates per balance line
	C-03A,B	Single-phase flow through the cold leg to CMT balance lines, four flow rates per balance line
	C-04A,B	CMT draindown using cold leg to CMT balance line
	C-05A,B	CMT gravity draindown using pressurizer to CMT balance line
	C-06A,B	SI accumulator blowdown
	C-07A,B	IRWST gravity draindown, three water levels
	C-08	CVS, RNS, and SFWS pump flow rate verification
	C-09	Operation of primary system with two RCPs running
	C-10A,B	Operation of primary system with one RCP running
Hot shakedown tests	H-01	Facility heated and heat at five constant temperatures
	H-02	Starting from nominal conditions, power will be shut off and SGs isolated
	H-03	Facility operated at normal full-pressure, temperature, and power
	H-04	Facility transitioned from full power operating conditions to hot shutdown/natural circulation mode of operation
	H-05	Low-pressure safety system actuation using the ADS with CMT draindown and accumulator delivery
	H-06	Full-power, full-pressure safety system actuation initiated by the opening of the first stage of the ADS

Table A.1-5 Matrix Tests, Full-Pressure, Full-Height Integral Systems Test (SPES-2) (cont.)

Test Number	Description
3	2-inch cold leg break with nonsafety systems off
1	1-inch cold leg break with nonsafety systems off
4	2-inch cold leg break with nonsafety systems on
5	2-inch DVI line break with nonsafety systems off
6	DEG break of the DVI line with nonsafety systems off
7	2-inch break of cold leg to CMT balance line with nonsafety systems off
8	DEG break of cold leg to CMT balance line with nonsafety systems off
9	Design basis SGTR with nonsafety systems on and operator action to isolate SG
10	Design basis SGTR with nonsafety systems on and no operator action
11	Design basis SGTR with manual ADS actuation
12	Large SLB

Table A.1-6 Matrix Tests, Full-Pressure Integral Systems Test (ROSA-AP600)		
No.	**Test**	**Test Description**
1	AP-CL-03	1-Inch Bottom-Oriented Cold Leg (CL) SBLOCA[1]. SPES configuration & ADS Stages 1, 2, 3 One-Valve Operation.
2	AP-AD-01	Inadvertent Opening of ADS Stage[1]. SPES configuration.
3	AP-CL-04	1/2-Inch Bottom-Oriented CL SBLOCA[1]. AP600 configuration.
4	AP-PB-01	2-Inch Pressure Balance Line (PBL) SBLOCA[1]. SPES configuration.
5	AP-CL-05	1-Inch Bottom-Oriented CL SBLOCA with Failure of ADS Stages 1, 2, & 3. AP600 configuration.
6	AP-PB-02	1-Inch PBL SBLOCA, P-Loop CMT Check Valves Failed Closed, C-Loop Loop Seal Bypass Open. AP600 configuration.
7	AP-DV-01	Direct Vessel Injection (DVI) Line Double-Ended-Guillotine Break (DEGB)[1]. AP600 configuration with revised coolant pump coastdown.
8	AP-CL-06	1-Inch Top-Oriented CL SBLOCA[1]. SPES configuration & ADS Stages 1, 2, 3 One-Valve Operation.
9	AP-BO-01	Station Blackout[1,2]. AP600 configuration with revised coolant pump coastdown.
10	AP-SG-01	Steam Generator Tube Rupture (SGTR): 1-3/4 Tubes Ruptured[1]. AP600 configuration with revised coolant pump coastdown.
11	AP-SL-01	Main Steam Line Break with 5-Tube SGTR[1]. AP600 configuration.
12	AP-CL-07	1-Inch Bottom-Oriented CL SBLOCA with Failure of 75 percent of ADS Stage 4 (Only 25 percent of ADS Stage 4 in C-Loop)[3,4]. SPES configuration & ADS Stages 1, 2, 3 One-Valve Operation.
13	AP-CL-08	2-Inch Bottom-Oriented CL SBLOCA[1,4,5]. AP600 configuration with revised coolant pump coastdown.
14	AP-CL-09	1-Inch Bottom-Oriented CL SBLOCA with Chemical Volume Control System (CVCS) Makeup Pump Injecting Into P-Loop Crossover Leg, 1 Accumulator (P-Loop), No CMTs, 50 percent of ADS, & 1 of 2 IRWST Gravity Drain Lines (P-Loop). AP600 configuration with revised coolant pump coastdown.

[1]One Stage 4 ADS valve failed in C-Loop.
[2]Core power decay curve includes G-Factor henceforth.
[3]PRHR heat exchanger bundle reduced from 45 tubes to 21 tubes.
[4]Steam separators installed on ADS Stage 4 discharge lines.
[5]IRWST Feed & Bleed system used.

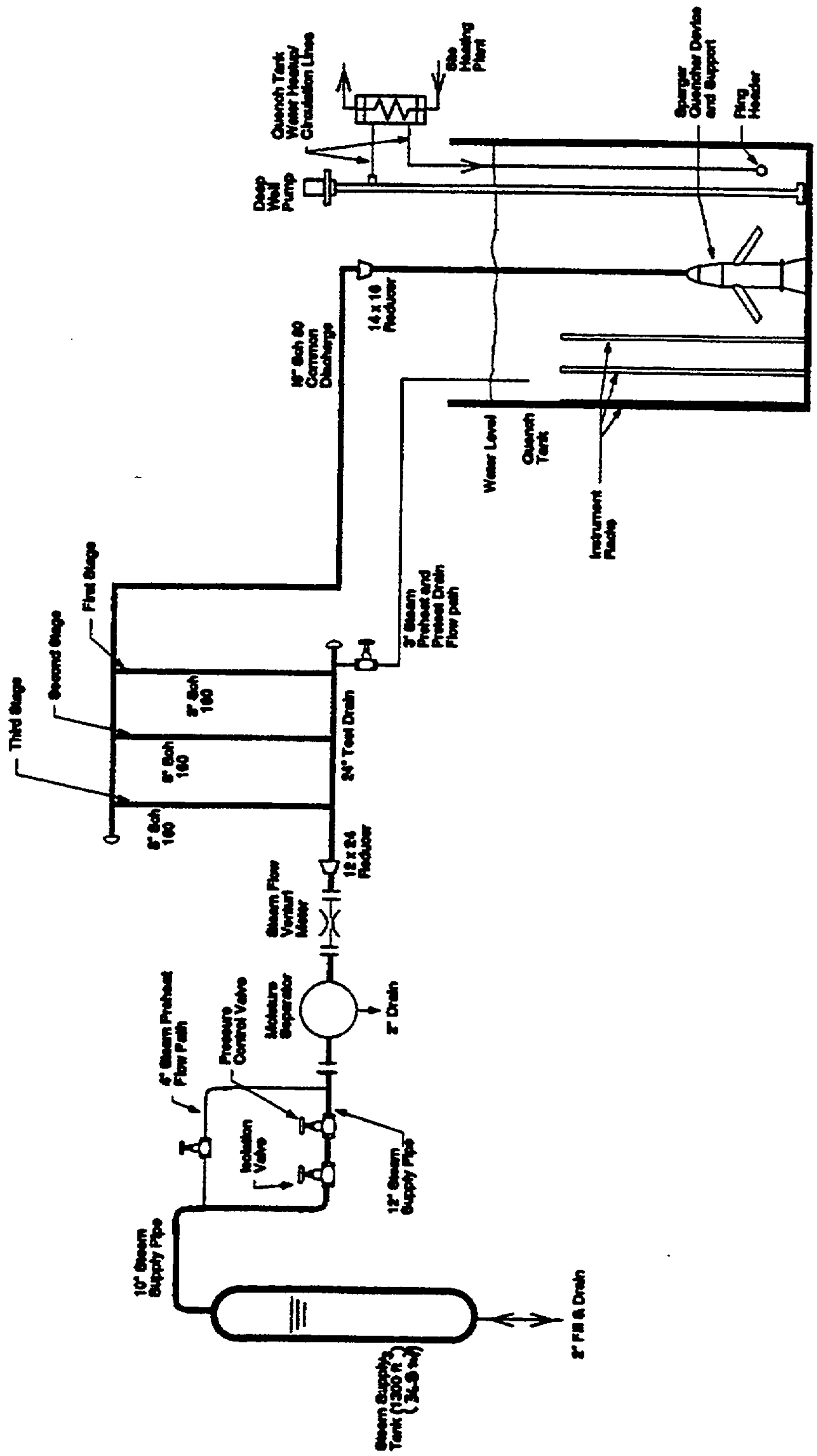

Figure A.1-1 ADS Phase A Test Facility

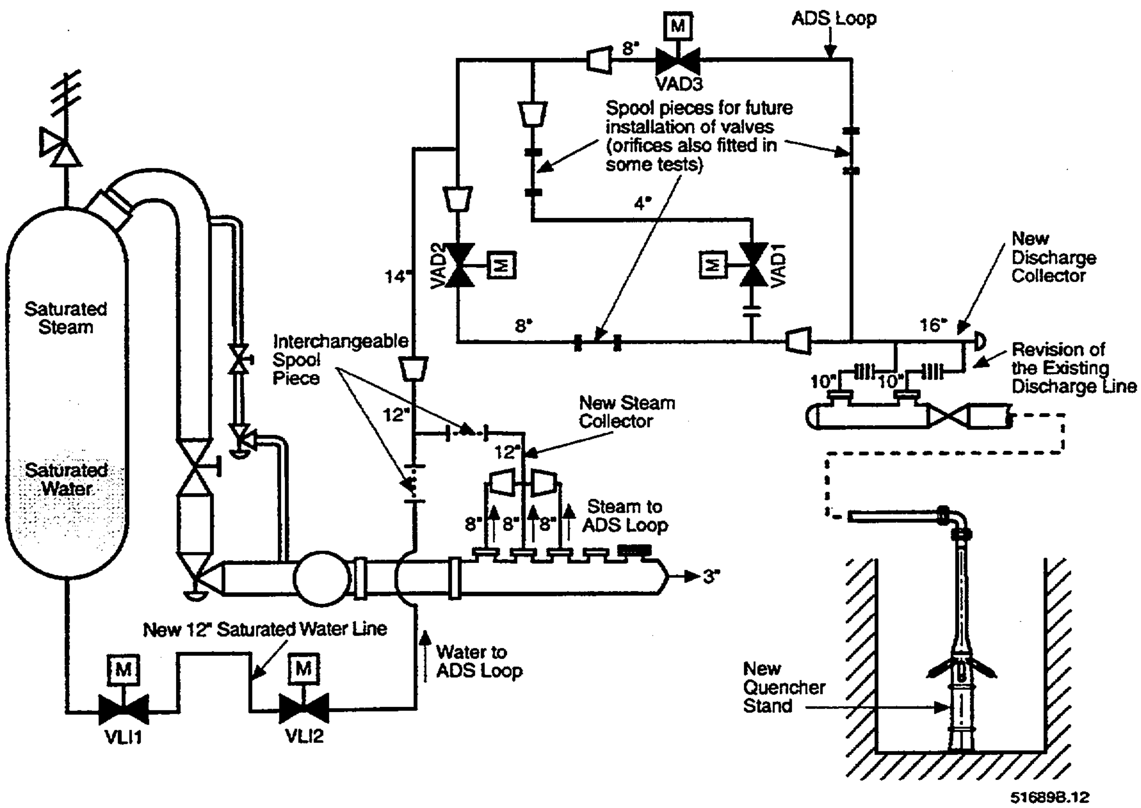

Figure A.1-2 ADS Phase B Test Facility

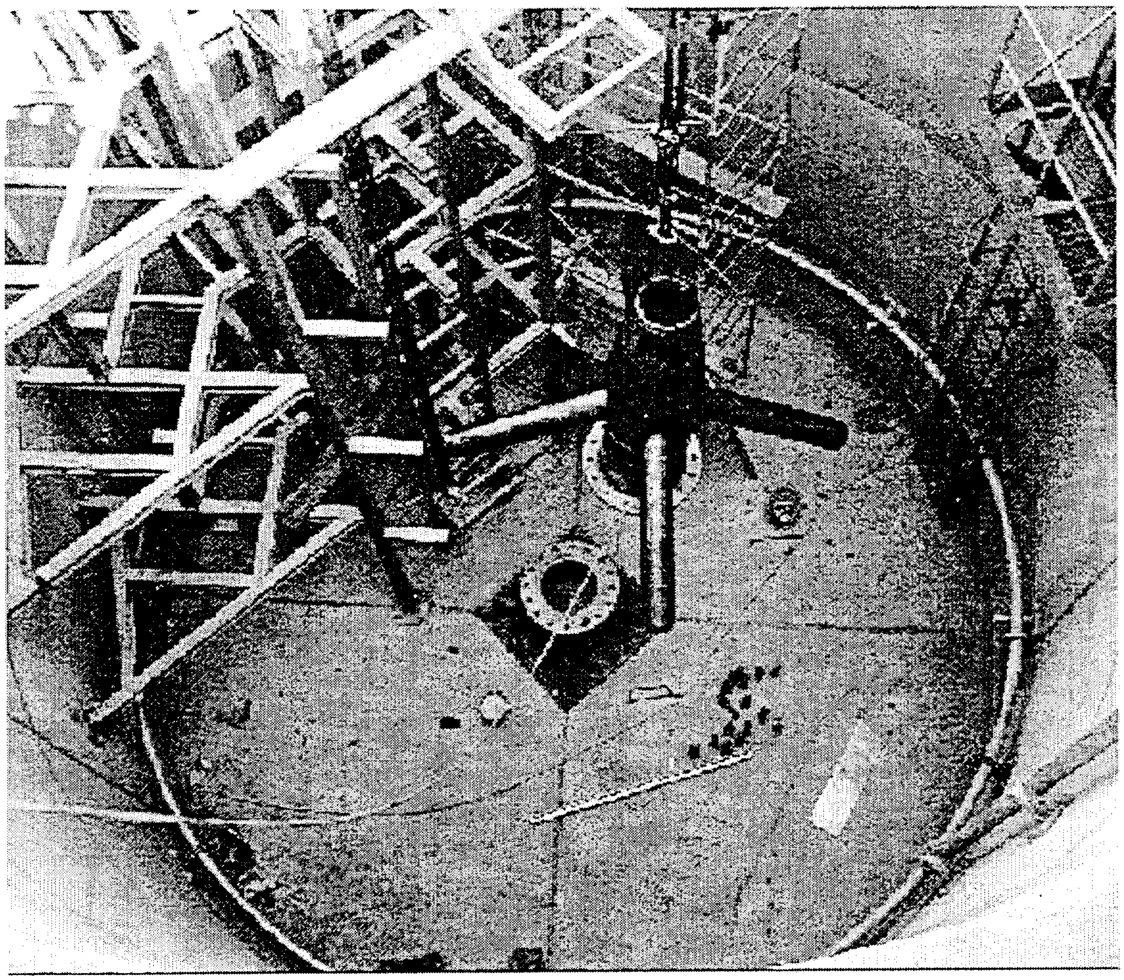

Figure A.1-3 ADS Test Facility – Prototypic Sparger in Quench Tank

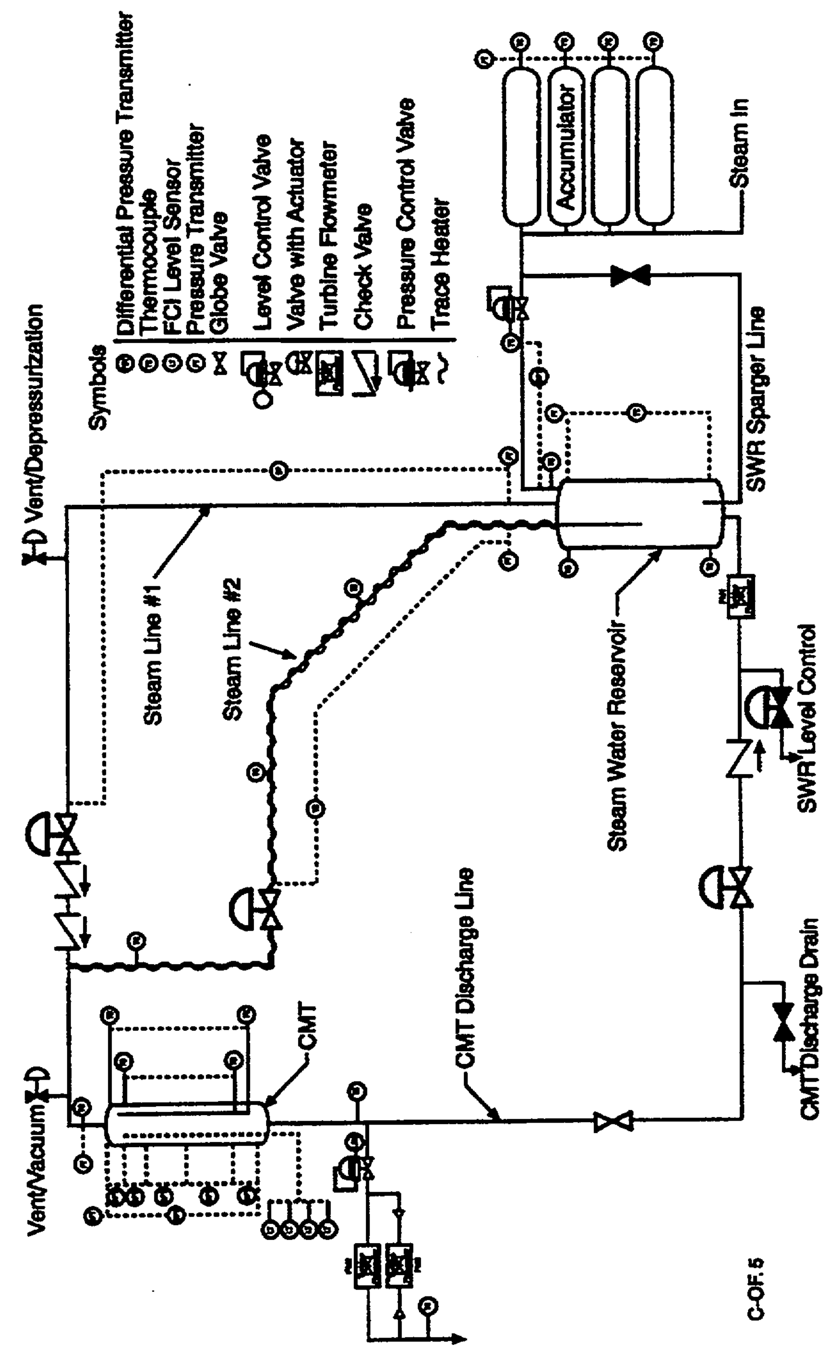

Figure A.1-4 CMT Test Facility Schematic

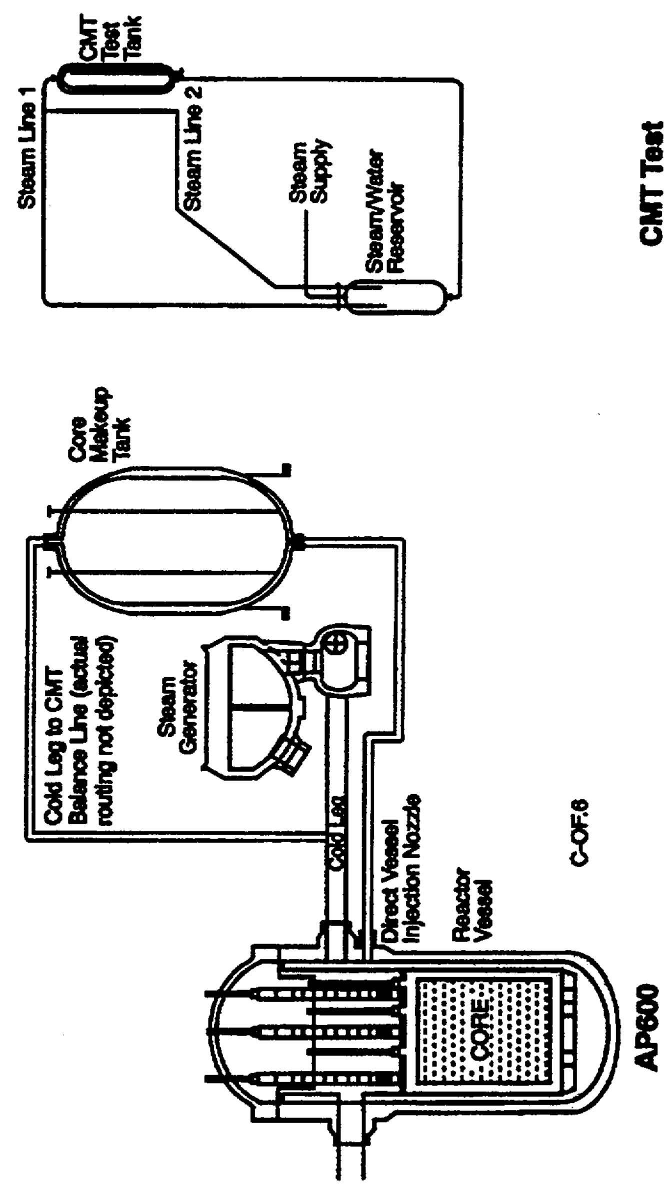

Figure A.1-5 AP600 CMT and RCS Layout and CMT Test Tank and Steam/Water Reservoir

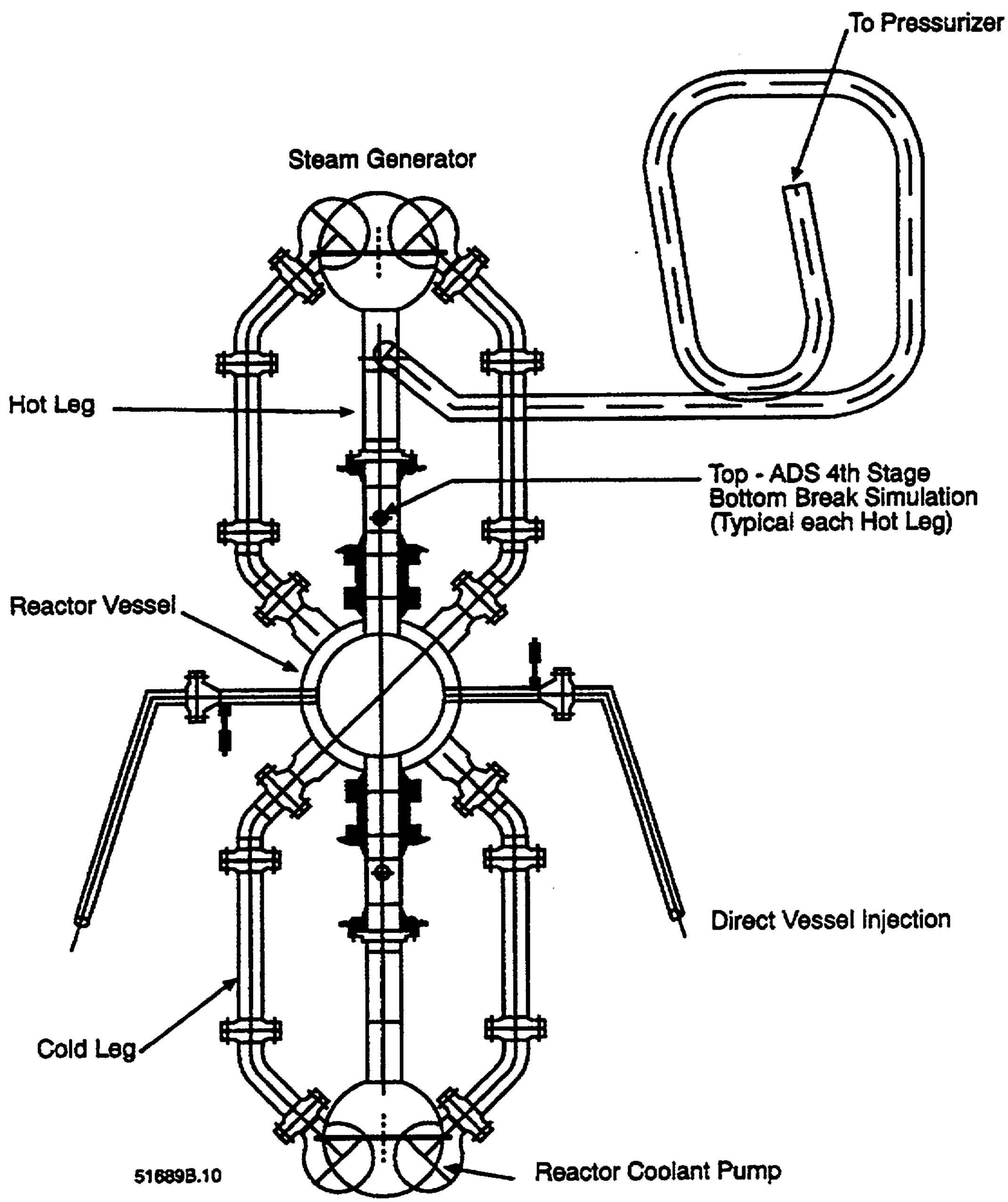

Figure A.1-6 OSU Test Facility Primary System Schematic

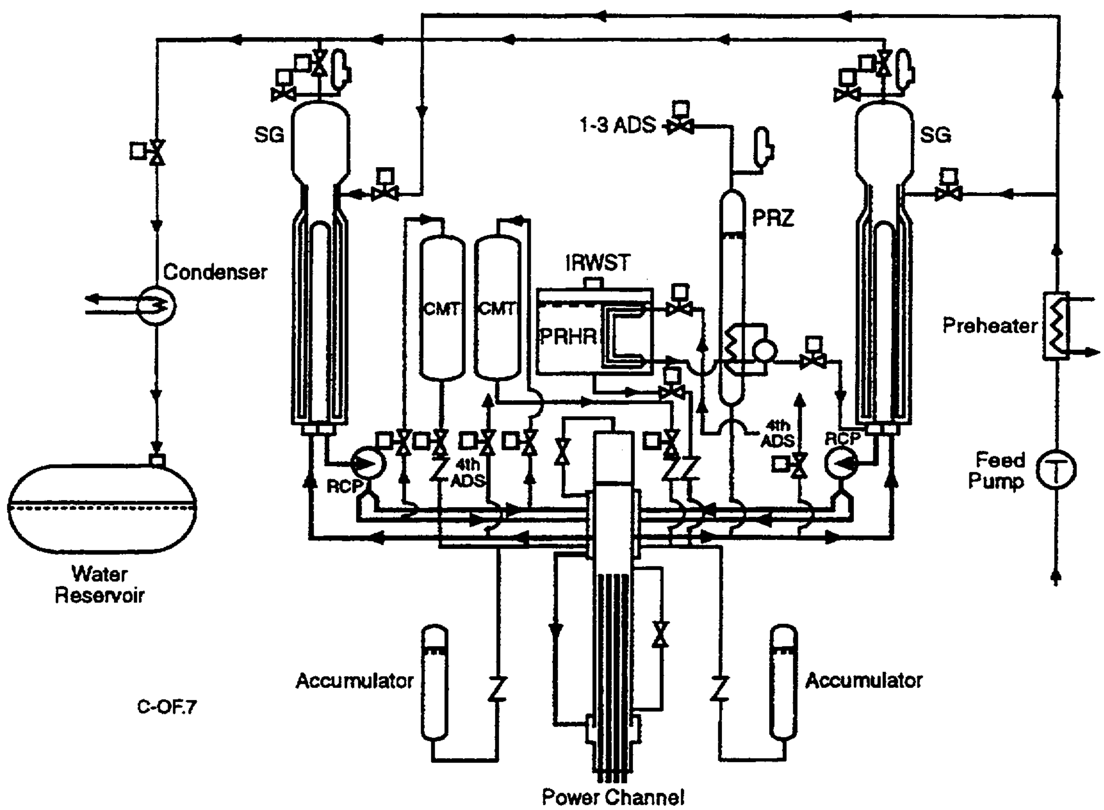

Figure A.1-7 SPES-2 Facility Primary System

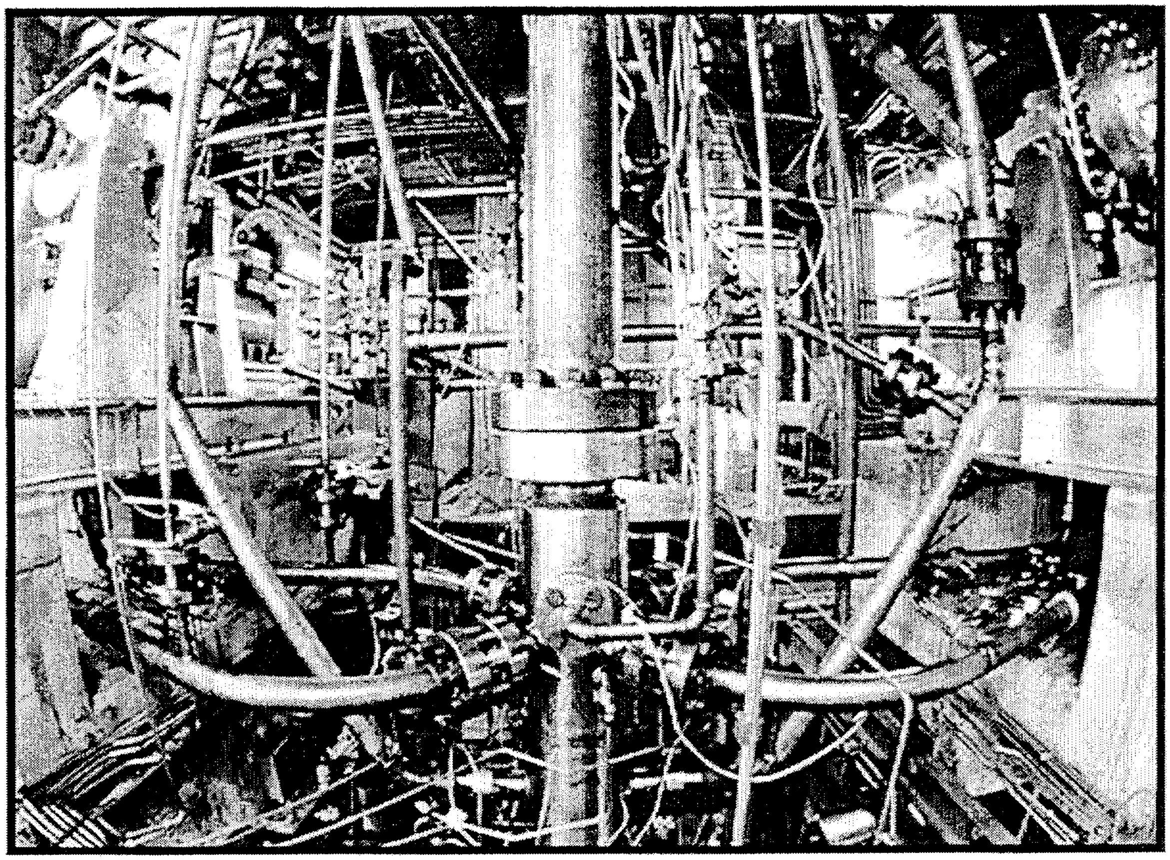

Figure A.1-8 SPES-2 Facility Upper Portion of Reactor Vessel

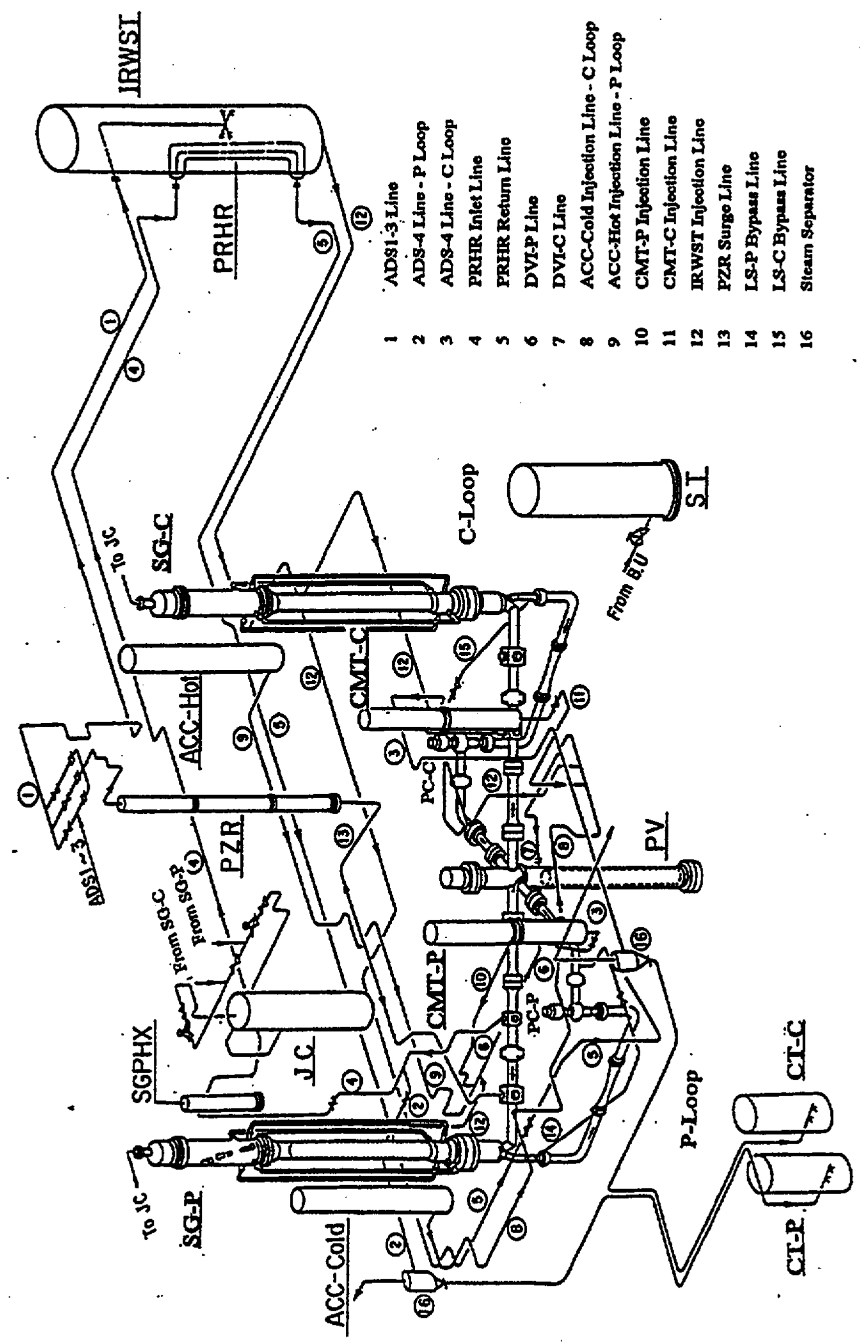

Figure A.1-9 ROSA-AP600 Schematic

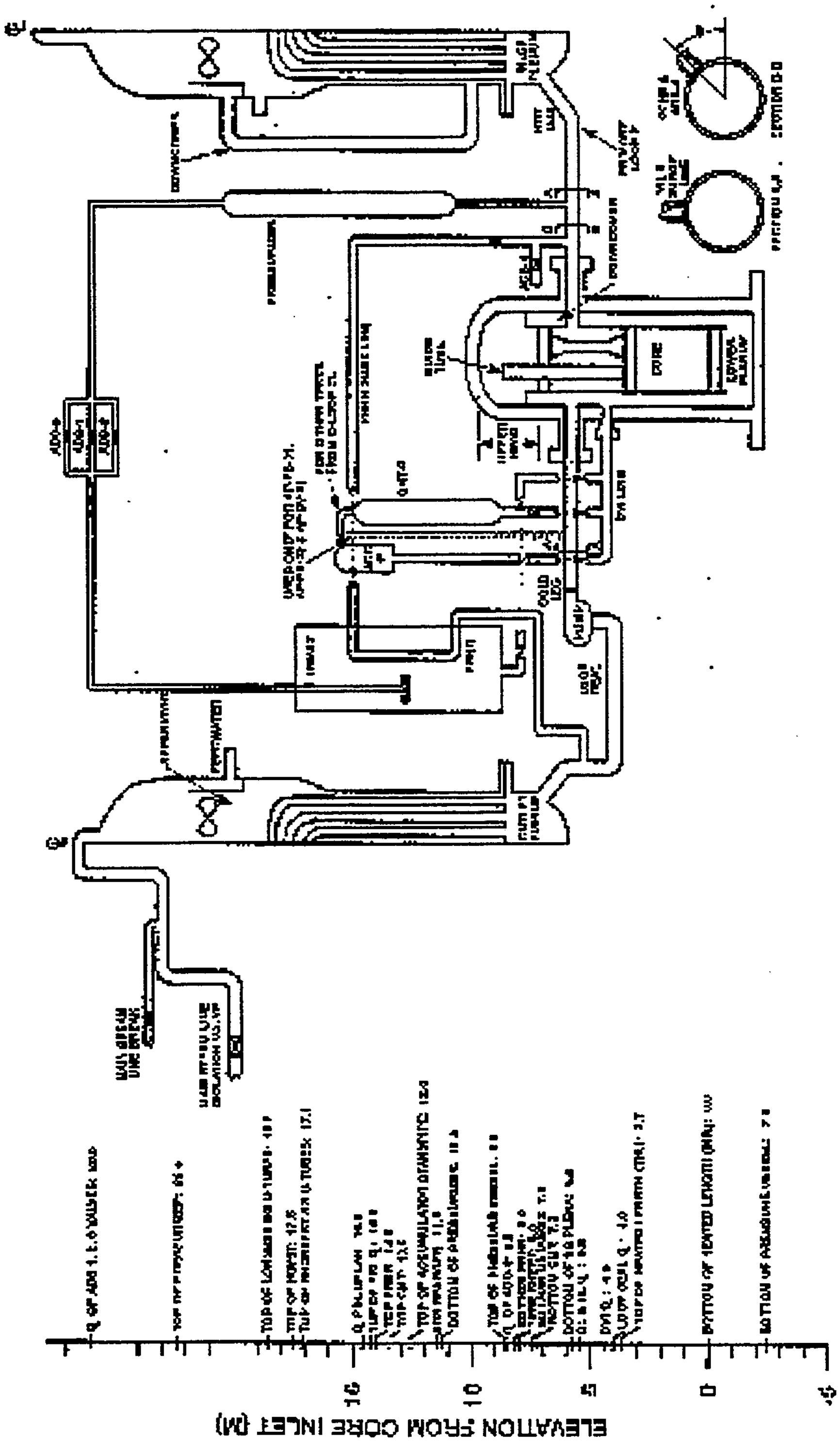

Figure A.1-10 ROSA-AP600 Elevations (Sheet 1 of 2)

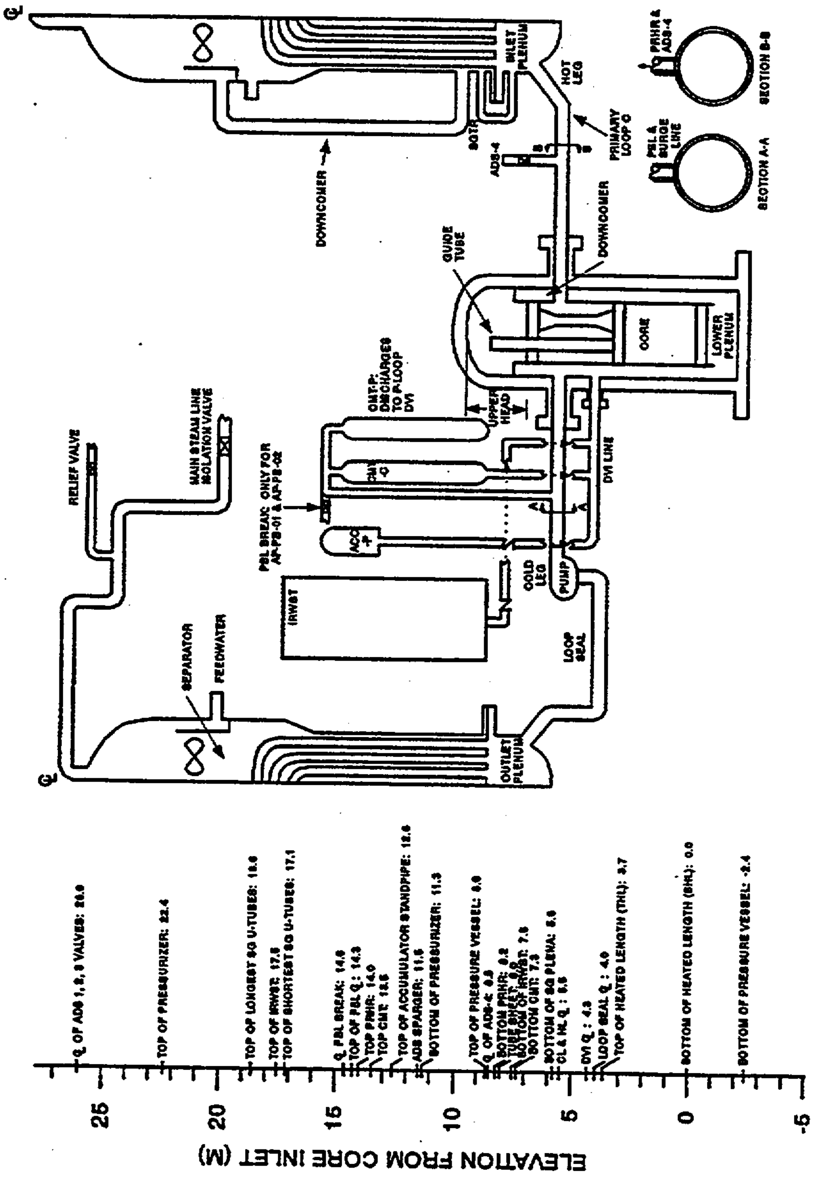

Figure A.1-10 ROSA-AP600 Elevations (Sheet 2 of 2)

A.2 PASSIVE CONTAINMENT COOLING SYSTEM (PCS) TEST SUMMARIES

The following tests were performed for the PCS.

- Air flow path pressure drop test (subsection A.2.1)
- Water film formation test (subsection A.2.2)
- Wind tunnel bench experiment (subsection A.2.3)
- Condensation test (subsection A.2.4)
- PCS water distribution test (subsection A.2.5)
- PCS wind tunnel test (subsection A.2.6)
- Heated plate test (subsection A.2.7)
- Integral PCS test (subsection A.2.8)
- Large-scale integral PCS test (subsection A.2.9)

A.2.1 Air-Flow Path Pressure Drop Test

A one-sixth scale replica of a 14-degree section of the entire PCS air-flow path was constructed to quantify the air-flow path resistance, determine if aerodynamic improvements were needed, and demonstrate the effectiveness of these improvements (Figure A.2-1).

The air-flow path was constructed of heavy plywood and sheet metal and used a blower at the outlet diffuser end to draw air through the model. The air-flow baffle surrounding the vertical sides of containment (downflow inlet/upflow outlet air flow divider wall) was modeled to reflect the corrugated sheets, reinforce and support beams, and support posts that maintain separation between the shield wall and hold the baffle and containment. The air flow above containment accurately modeled the PCS water storage tank support beam flanges, steel radiation shielding plates, wire grill, and chimney structure. The air flow Reynolds numbers were maintained below the scaled Reynolds number that would correspond to the actual design, throughout testing, to ensure that the measured f(L/D)s were conservative.

Instrumentation consisted of a series of wall pressure taps located throughout the air-flow path of the model. Each was located in the center of the air-flow path with care taken to maintain a smooth surface where penetrating the wall. The taps were connected to a pressure transducer via an electrically driven scanning valve. The voltage output of the transducers was measured and recorded at regular intervals by a data acquisition system (DAS). Flow velocities were measured using a wedge probe with both wedge side taps connected together.

Test Matrix/Results

The initial test results showed that the turning and inlet flow losses at the 180-degree turn into the bottom of the containment annulus and the losses in the containment annulus were the largest pressure losses. Therefore, several modifications were made:

- A rounded inlet was added at the containment annulus inlet.

- Since the turning radii for some streamlines at the annulus inlet would be relatively small, the rounded inlet was constructed using perforated metal to minimize flow separation.

- The air baffle sheet corrugations were made wedge-shaped at the inlet to lessen the tendency to contract the flow.

- The support posts from containment to the baffle were streamlined by adding fairings.

The results of this test showed that the total PCS air cooling path pressure loss coefficient was reduced by 45 percent by adding the streamlining features. This reduced loss coefficient was used in subsequent analyses of PCS performance.

Pressure drop in the air-flow path was quantified for the PCS. This test for the AP600 demonstrated that the pressure coefficients in the air flow could be estimated, verified, and improved with simple design changes.

A.2.2 Water Film Formation Test

General Description/Purpose

A survey of coatings that could be used on the AP600 containment was conducted to determine a coating that would provide corrosion protection and could be conducive to establishing a stable water film on the containment exterior surface. After selection of a coating candidate, a simple qualitative test was performed to demonstrate the wetability of the prototypic paint selected for use on the containment outer surface, and to characterize general requirements for forming a water film over a large surface area. The test apparatus consisted of a flat steel plate, 8 ft long in the flow direction and 4 ft wide. The plate was pivoted so that it could simulate nearly horizontal sections of the dome as well as the vertical containment sidewalls.

Test Matrix/Results

Water flow was supplied to the plate at a single point at the top center edge of the plate and was measured to simulate actual plant flow conditions. Various flow spreading devices were tried both to induce and observe uniform film behavior and to judge spreading requirements.

Summarized results of the test are:

- The selected paint readily wetted and rewetted after being dried.

- No rivulet formation was observed on this painted surface even at high point source flow rates and vertical orientation.

- With a point source of water, without additional distribution, most of the flow was in a 12-in. wide path down the 8-ft length.

- Several methods were able to create a water film across the entire width of the plate at various flow rates. Once formed, this water film was stable, did not form into rivulets, and wetted the entire length of the plate surface.

These results, combined with additional observation of film behavior in the tests described in subsections A.2.3 and A.3.5, were used to devise appropriate water distribution devices applicable to the actual containment structure.

A.2.3 Wind Tunnel Bench Experiment

General Description/Purpose

Bench wind tunnel tests of the PCS were conducted at the Westinghouse Science and Technology Center using 1/100-scale models of the AP600 shield building, air inlets and outlets, annulus baffle, and containment. These tests were performed to establish the proper location of the air inlets and to confirm that wind will always aid containment cooling air flow. Two models were used: one consisted of only the shield building and diffuser discharge without inlets and internal flow; the second included the air inlets, air baffle, containment, tank support structure, and a fan to simulate convective air flow. Pressures were measured at the inlet, building side and top, bottom of inlet annulus, top of containment at the discharge of the air baffle, and in the chimney. Air flow was measured at the inlet to the containment baffle.

Test Matrix/Results

These tests were run with a uniform wind tunnel air velocity of 85 ft/sec. Test Reynolds numbers for the shield building and chimney were demonstrated to be in the transition region. The models used in this test were 10-inches in diameter and 18-inches in overall height. The model that included the containment and air baffle structures was instrumented with static pressure taps (SPTs) and an air velocity (anemometer) measurement. The instrumentation was located in a common vertical plane, and the model was rotated 360 degrees to obtain the air pressure profile around the entire structure.

The results from this test showed that when the air inlets are located on the top (roof) of the shield building, a "chimney" effect was created over a significant portion of top of the building (this effect became more pronounced when the wind direction was inclined upward), while air inlets located at the top of the shield building sidewalls overall provide the most positive wind-induced driving pressure versus air exit pressure.

Air pressure profiles in the shield building across the cooling air baffle to the air exit with external wind were developed. By comparison to a "no-wind" case where all the cooling air flow was induced by the fan, it was shown that, with the selected air inlet arrangement, the wind will always increase the containment cooling air-flow rate.

Other significant conclusions from this test were:

- Deep beams behind the air inlets (as provided in the PCS water storage tank structure in the original shield building design) significantly increased wind-induced containment air cooling flow.

- Containment air cooling flow was insensitive to wind direction and to a 15-degree downward wind inclination. Cooling flow was increased by a 15-degree upward wind inclination.

A.2.4 Condensation Test

General Description/Purpose

A series of condensation experiments to examine, in detail, condensation of air/steam mixtures flowing over cold surfaces were performed under Westinghouse funding to the University of Wisconsin. These experiments were used to develop improved models for the containment interior heat transfer.

Test Matrix/Results

The first series of tests examined condensation over a horizontal surface, as a reference. The next series of tests inverted the condensing surface so that it modeled the inside of the containment dome and sidewalls. The condensation rates were more than twice that of a flat horizontal surface. Finally, these experiments were rerun using a specially prepared surface coated with the same paint used inside containment for corrosion resistance. The condensation was reduced, but was still twice that for a horizontal surface.

These small-scale, well-instrumented tests provided the basis for computer code model improvements, so that the AP600 containment interior heat transfer performance could be accurately predicted.

A.2.5 PCS Water Distribution Tests

General Description/Purpose

The PCS water distribution test was conducted to provide a large-scale demonstration of the capability to distribute water on the steel containment dome outer surface and top of the containment sidewall. The overall objectives of the PCS water distribution test were to quantify the effectiveness of the water distribution over the containment dome and top of the containment sidewall, and to provide data to finalize the design of the AP600 containment water distribution. The results of the tests were used in the safety analysis of the AP600 containment response.

The test was conducted in several phases. Phase 1 utilized a full-scale simulation of the center of the containment dome out to the 10-ft radius. The surface of the model was coated with the prototypic AP600 containment coating. The test was used to evaluate water delivery to the dome. Water distribution measurements were obtained by collecting and measuring flow off the periphery of the model. In addition, the test evaluated the use of a surfactant to promote water film formation.

Phase 2 was conducted on a full-scale 1/8 sector of the containment dome at the Westinghouse Waltz Mill facility located in Madison, Pennsylvania. The phase 2 test modeled both the AP600 water supply and a distribution system arrangement. The surface of the test model incorporated the maximum allowable weld tolerances between the steel plates and was coated with the prototypic AP600 containment coating to provide similarity to the AP600 plant design. Measurements of the water distribution were obtained by collecting and measuring the flow over defined areas and by selective measurement of film thicknesses using a capacitance probe. In addition, the test evaluated the use of a surfactant to promote water film formation.

Phase 3 was used to confirm the final design of the water distribution system. Measurements of the water distribution were obtained by collecting and measuring the flow over defined areas and by selective measurement of film thicknesses using a capacitance probe. The results of the phase 3 test were compared with the phase 2 results to verify the performance of the final water distribution system design.

Test Matrix/Results

Phase 1 tests were conducted over a range of water flow rates that bracketed the anticipated flows. Tests were also conducted with and without any distribution devices and with imposed surface tilts.

Phase 2 tests were also conducted both with and without prototypic spreading devices at flow rates, which simulated the expected water delivery from flow initiation to the 3-day delivery rate. As with the tests from phase 1, phase 2 tests showed a more even distribution with increasing flow rate. At high flow rates, water distribution on the dome was greater than 65 percent. At low flow rates, the coverage decreased to below 40 percent. The test also re-affirmed the need for a water distribution device on the containment dome.

Phase 3 tests were completed and used to verify the performance of the finalized distribution device design. The matrix for phase 3 testing was provided in Table A.2-1.

A.2.6 PCS Wind Tunnel Tests

General Description/Purpose

The PCS wind tunnel test was conducted primarily in a boundary layer wind tunnel at the University of Western Ontario. The overall objectives of the PCS wind tunnel test were to demonstrate that wind does not adversely affect natural circulation air cooling through the shield building and around the containment shell and to determine the loads on the air baffle. The test was conducted in four phases (1, 2, 4A, and 4B).

Phases 1 and 2 were conducted with a 1/100-scale model of the AP600 shield building and surrounding site structures, including the cooling tower. The model of the shield building and surrounding structures was placed in the tunnel on a turntable, which permitted the entire assembly to be rotated to simulate the full 360 degrees of wind directions. The wind tunnel also allowed extended fetches of coarsely modeled upstream terrain to be placed in front of the building under test. The wind tunnel flow (about 75 ft/sec) then developed boundary layer characteristics representative of those found in full scale. For this testing, a boundary layer representative of open-country conditions (ANSI C) was developed.

Phase 1 modeled the site structures and external shield building only. No internal flow passages were provided. The shield building model was instrumented with pressure taps at the inlet locations and in the chimney. The purpose of phase 1 was to compare the pressure coefficients developed following changes to shield building and/or site structures with the pressure coefficients developed on the current plant design. Note that the base case was without the cooling tower.

Phase 2 used the model from phase 1 testing, modified to include a representation of the shield building air-flow path. The shield building model was instrumented with pressure taps inside the inlet plenum and in the chimney. In addition, pressure taps were located throughout the air-flow path to provide for approximate baffle wind loads at several locations. The purpose of phase 2 was to explore the effects of the flow path on the developed pressure coefficients and to determine wind loads on the air baffle.

Phase 3 was planned to provide an estimate of the amount of effluent that would be recirculated from the chimney of the shield building to the inlets. This phase of testing was cancelled.

Phase 4A was conducted at both the University of Western Ontario and the Canadian National Research Council's (CNRC's) wind tunnel in Ottawa, Ontario, on both the 1/100-scale model and a 1/30-scale model. The primary objectives of the test were to confirm that the detailed phase 2 results at the University of Western Ontario conservatively represented those expected at full-scale Reynolds numbers and to obtain better estimates of baffle loads in the presence of a cooling tower.

The first portion of phase 4A was conducted at the University of Western Ontario using the existing 1/100-scale model of the shield building and site-surrounding structures. Additional instrumentation was added to the model to provide useful overall comparison of Reynolds number effects between the tests at the two facilities. For comparative purposes, the model was equipped with a sealing plate at the interior base of the chimney to prevent flow through the interior passages, when desired. Tests were also conducted with the flow path open in a uniform wind field to provide true instantaneous baffle loads for a tornado case.

The phase 4A tests at CNRC were conducted on a 1/30-scale model of the shield building. The model did not have complete internal passages; however, the chimney was open inside to its base, and a simple inlet manifold was included extending just below the inlets. This was connected to an additional internal volume designed to compensate for the frequency response of the volume of the blocked passages in the 1/100-scale model. Instrumentation on the model was similar to the 1/100-scale model on the exterior and inside the chimney to provide comparative results between the tunnels. A 1/100-scale model of the cooling tower was tested in the CNRC tunnel to provide a cooling tower waste pressure distribution and wake properties for application in the phase 4B testing.

The objectives of the phase 4B tests were to explore variations in site layout and topography to determine whether or when such variations significantly affect the net pressure difference between the inlet and chimney of the AP600 and, by implication, the convected flow and net baffle loads. A small-scale model of the site buildings and local topography was built at a scale of about 1/800. This scale range ensured that both the reactor and cooling tower models were in the same Reynolds number range (subcritical), while remaining a size that allowed the use of straightforward modeling and instrumentation techniques.

Test Matrix/Results

The data from the phase 1 base case design indicated a significant positive pressure difference between the inlets and the chimney. Changes to the inlets only marginally reduced the pressure difference. Raising and lowering the chimney had little effect. Raising and lowering the turbine building also had little effect. The presence of the natural draft cooling tower significantly increased the turbulence at the shield building, resulting in larger fluctuating differential pressures. However, in all cases, the mean pressure difference remained positive. Removal of the deaerator from the turbine building roof showed no effect.

The majority of the tests for phase 2 were conducted at one wind angle with all site structures except the cooling tower. Pressure coefficients were measured across the baffle. Mean pressures from all taps on a particular level were compared to examine the uniformity of the pressures around the baffle. The data indicated that the distributions were fairly uniform, even at the top of the annulus. The presence of the cooling tower increased the pressure fluctuations, but the mean remained about the same.

The phase 4A tests at CNRC verified that the tests at the University of Western Ontario were independent of Reynolds numbers.

Phase 4B site geography testing conducted at the University of Western Ontario consisted of the following cases:

- A reference case–consisting of the current site layout, including all site buildings and a cooling tower on flat open-country terrain

- A series of other cases–idealized sites based on Diablo Canyon and Trojan and/or Indian Point

- The Diablo Canyon type site addressed speedup due to an escarpment. The Trojan/Indian Point site looked at the effects of a river valley site.

A.2.7 PCS Heated Plate Test

General Description/Purpose

In the PCS concept, heat transfer from the outside of the vessel was performed by forced convection heat transfer from the steel containment surface to air (including some radiation to the divider wall) and evaporation of a water film on the wetted outside area of the containment surface above the operating deck elevation. In order to obtain data for the heat and mass transfer processes, and to observe film hydrodynamics including possible formation of dry patches due to surface tension instabilities, experiments were performed on a thick steel plate heated on one side and with an evaporating water film and ducted air flow on the other side.

The experimental apparatus consisted of a 6-ft long, 2-ft wide, and 1-in. thick steel plate coated with the same coating planned for use on the containment vessel. An air duct was formed over the plate by side walls and a Plexiglas cover for flow visualization. A four-speed blower ducted through a set of turning vanes provided air-flow velocities which simulated the full range of both natural draft in the containment cooling duct and flows induced by a high wind. Water, preheated in an automatically controlled water heater, was supplied at a metered rate to a simple distributor located at the upper end of the plate.

To simulate the heating of the containment wall that would occur in an actual plant following a postulated accident, the test plate was heated from the back side using a high temperature heat transfer fluid, UCON*500. The heat transfer fluid flowed through copper heating tubes that were soldered into grooves in the back of the plate. The heat transfer fluid was electrically heated in a drum with an automatic temperature control and pumped through a flow meter to the tube inlet manifold. All hot parts, except the front of the plate, were insulated to minimize heat loss.

The plate could be placed in a vertical position to simulate the containment side wall or inclined somewhat from horizontal to simulate the different slopes on the elliptic containment dome. Plate temperatures and heat fluxes were measured at six locations by pairs of thermocouples. In addition, air inlet and outlet temperatures were measured together with duct velocity. An electronic watt meter registered total heater power. Water outlet flow and temperature were also measured. Temperature and power data were recorded on a data acquisition system.

Test Matrix/Results

Experiments were performed with no water on the plate and for a range of water film flow rates simulating the high water flow on the upper part of containment down to the lower part of containment where the water was nearly completely evaporated at the high heat flux. A series of tests to isolate and observe the effect of air velocity at one representative film flow was completed. Tests at high air velocities were performed to examine the high wall shear effects for a number of film flow rates. A limited set of tests was performed at 15-degree inclination to horizontal to provide data for the thicker films that flow on the dome. A summary of test conditions is provided in Table A.2-2.

The evaporation rate of water from the heated plate was shown to agree with or exceed those expected and confirmed the overall heat transfer capability of the PCS concept. The following conclusions were drawn from the test results:

- Water film evaporation and resultant heat removal agreed with or exceeded expected values.
- Heat transfer from the water film to air was performed by forced convection plus mixing with hotter evaporated water vapor.
- Radiation to the air baffle wall and subsequent heat transfer to the cooling air occurred and accounted for some of the heat transfer.
- Heat transfer from containment to the air with no water film agreed very well with expected values.
- Water film flowing on the coated steel surface was wavy laminar flow not susceptible to instabilities that lead to dry patch formation at any heat flux density or plate surface temperature encountered.
- A water film was easily formed on the coated steel surface even in the vertical orientation. Once formed, the film showed no instability or tendency to form rivulets. This was true at all tested water flow rates.
- The water film was not adversely affected by the countercurrent cooling air flow up to the maximum air velocity of the test (e.g., no water-film stripping occurred).

A.2.8 Small-Scale Integral PCS Test

General Description/Purpose

This test simulated PCS heat transfer processes occurring on both the inside and outside containment surfaces. The test apparatus included a 3-ft diameter, 24-ft high steel pressure vessel internally heated by steam supplied at various pressures. A transparent wall around the pressure vessel was used to create a 15-inch wide annulus for fan-driven or natural circulation air flow. In order to simulate a full range of possible air temperatures and humidities, the incoming air was heated by a steam heating coil and humidified with steam. Instrumentation to measure internal steam condensing rates, external water evaporation rates, containment wall inner and outer temperatures, water film and air temperatures, humidities, and air velocities was provided. Speed control of the draft fan at the diffuser section permitted simulation of a full range of air-flow conditions in the air annulus.

Test Matrix/Results

The tests were conducted with varying steam supply flow rates, water film flow rates, inlet air temperatures, and inlet air humidities (Table A.2-3). Instrumentation was provided to measure internal steam condensation rates, external water evaporation rates, containment wall inner and outer temperatures, water film temperatures, air temperatures, humidities, and air velocities.

The following conclusions and observations were drawn from this test:

- The heat removal capability from the external surface of the test vessel for both wetted and dry conditions agreed well with previous heated plate experiments and analytic predictions and supported the AP600 containment analysis.
- The overall heat removal capability from the test vessel with a wetted surface and well-mixed air and steam inside agreed well with analytical predictions.
- The local heat removal rate at the top of the vessel where "cool" water was first applied was significantly higher than the vessel average heat removal rate.
- The water film behavior was stable and predictable even at evaporating heat fluxes three times higher than is likely to be encountered in actual application.
- A uniform water film was easily formed on the coated steel containment surface using simple weirs even after extended exposure to weather effects.
- The water film on the vertical side walls of the coated steel surface of the vessel had no tendency to become less uniform or form rivulets, so that no water film redistribution was required on the vertical walls.

A.2.9 Large-Scale Integral PCS Test

General Description/Purpose

The large-scale PCS test consisted of a 1/8-scale model of the AP600 containment in which both internal steam/air noncondensable gas conditions and external PCS operation were simulated in order to demonstrate the AP600 PCS heat transfer capability. The purpose of this test was to examine, on a large scale, the natural convection and steam condensation on the interior of the AP600 containment combined with exterior water film evaporation, air cooling heat removal, and water film behavior. The PCS heat transfer test results provided data for the verification of the computer model used to predict the containment response. Also, these test results combined with the PCS smaller-scale integral test provided insight on the ability of the computer model to predict results at two different test scales.

The test facility was located at the Westinghouse Science and Technology Center in Churchill, Pennsylvania. The facility consisted of a 20-ft high by 15-ft diameter pressure vessel with a 7/8-in. wall thickness (Figures A.2-2 through A.2-4) and the supporting hardware. The larger test vessel made it possible to study in-vessel phenomena such as noncondensable mixing, steam release jetting, condensation, and flow patterns inside containment. The vessel contained air or helium when cold and was supplied with steam for testing. A transparent acrylic cylinder installed around the vessel formed the air-cooling annulus. Air flow up (and/or water flow down) the annulus outside the vessel cooled the vessel surface, resulting in condensation of the steam inside the vessel. Superheated steam was throttled to a variable, but controlled, pressure and was supplied to the test vessel.

To establish the total heat transfer from the test vessel, measurements were recorded for steam inlet pressure, temperature, and condensate flow and temperature from the vessel. Thermocouples located on both the inner and outer surfaces of the vessel indicated the temperature distribution over the height and circumference of the vessel. Thermocouples placed throughout the inside of the vessel on a movable rake provided a measurement of the vessel bulk steam temperature as a function of position.

An axial fan at the top of the annular shell tested the apparatus at higher air velocities than can be achieved during purely natural convection. The temperature of the cooling air was measured at the entrance of the annular region and on exit of the annulus in the chimney region prior to the fan. The cooling-air velocity was measured in the cooling-air annulus using a hot wire anemometer.

The test facility provided the following critical data for the interpretation of the test performance:

- Containment wall heat flux measurements to provide local heat transfer rates
- Air baffle wall temperatures
- Vessel internal temperatures
- Air/helium concentration measurements
- Instrumentation to measure (to support a heat balance of) the PCS external air and water, and steam and condensate flows and temperatures

Test Matrix/Results

The large-scale PCS test was performed in two phases: baseline tests and confirmatory tests. The baseline tests were conducted to support the June 1992 AP600 SSAR submittal. The confirmatory tests were completed in November 1993 and are described in Table A.2-4.

Key results and observations for the PCS large-scale heat transfer test are:

- The heat removal capability from the external surface of the test vessel for both wetted and dry conditions agreed well with previous heated plate experiments and analytic predictions and supported the AP600 containment analysis.
- A uniform water film was easily formed on the coated steel containment surface using simple weirs even after extended exposure to weather effects.

- Helium mixed well inside the test vessel; no helium stratification was observed.
- The presence of helium had a negligible effect on heat transfer removal rates.
- Condensation and evaporation mass transfer were the only significant mechanisms for rejecting energy from containment to the PCS.
- Noncondensable distribution and internal velocity were important to the condensation rate.
- Tests simulating LOCAs show that internal velocities are sufficiently low, free convection dominates, and momentum does not carry from above to below the simulated operating deck.
- Tests simulating MSLB events show that internal velocities are significant, mixed convection exists, and momentum is transported from above to below simulated operating deck (which induces uniform concentrations).

Table A.2-1 Water Distribution Test, Phase 3

Test	Test Number	Description
Weir performance tests	1	Test of weir performance with initial water flow rate
	2	Test of weir performance with 24-hour water flow rate
	3	Test of weir performance with excessive water flow rate
	4	Test of weir performance with 3-day water flow rate
	5	Test of tilted weir performance with initial water flow rate
	6	Test of tilted weir performance with 3-day water flow rate
	7	Test of weir performance with initial water flow rate and plugged drainage holes
	8	Test of weir performance with initial water flow rate and plugged drainage holes
	15	Test of weir performance with initial water flow rate and baffle support plates
	16	Test of weir performance with 3-day water flow rate and baffle support plates
Film thickness tests	9	Test to measure film thickness and flow rate at initial water flow rate
	10	Test to measure film thickness and flow rate at 3-day water flow rate
	11	Test to measure film thickness and flow rate at excessive water flow rate
	12	Test to measure film thickness and flow rate at 24-hour water flow rate
	13	Test to measure film thickness with tilted weir and initial water flow rate
	14	Test to measure film thickness with tilted weir and 3-day water flow rate

Table A.2-2 Test Conditions, Test No., and Average Heat Flux (Btu/hr-ft²)

Water Film Flow Rate lbm/hr/ft of nominal	Air Velocity (ft/sec)						
	5.9	12.4	18.8	23.7	28.5	33.2	38.7
	Dry Plate Tests, Vertical Except 15 Degrees from Horizontal						
0		1	2	4	5	6	7
		680	860	930	1040	1100	1210
			3* 420				
	Water Film (Except Partially Dry) on Vertical Plate						
15	8 3120		9 3270				
60		10 3490	11 3640 12 2120				
110	13 3340	14 3610	15 3540 16 3580	18 3570	19 3670	20 3670	21 3650
170			17 3490				
310		22 3520	23 3570 24 2030				
			25 3560	26 3530			
	Water Film on Plate 15 Degrees from Horizontal						
60			27 3500 2800 1960				
110		29 3580	30 3590 31 2020				
310		32 3510					

Table A.2-3 AP600 PCS Small-Scale Integral Test Matrix

Test No.	Steam Outlet	Steam/Air Pressure (psig)	Cooling Air Velocity (ft/sec)	Water Film Flow (gpm)	Cooling Air Temp (°F)	Air Relative Humidity
1	Uniform	10	8	0	Ambient	Ambient
2	Uniform	20	8	0	Ambient	Ambient
3	Uniform	30	16	0	Ambient	Ambient
4	Uniform	40	16	0	Ambient	Ambient
5	Uniform	10	16	2.5	130	Ambient
6	Uniform	30	16	2.5	130	Ambient
7	Uniform	40	16	2.5	130	Ambient
8	Uniform	10	16	2.5	130	95°F wet bulb
9	Uniform	20	16	2.5	130	95°F wet bulb
10	Uniform	30	16	2.5	130	95°F wet bulb
11	Uniform	40	16	2.5	130	95°F wet bulb
12	Uniform	10	8	2.5	130	Ambient
13	Uniform	20	8	2.5	130	Ambient
14	Uniform	20	8	2.5	130	95°F wet bulb
15	Uniform	10	8	1.0	130	Ambient
16	Uniform	20	8	1.0	130	Ambient
17	Uniform	30	16	4.0	130	Ambient
18	Uniform	40	16	4.0	130	Ambient
19	Uniform	10	8	1.0	130	95°F wet bulb
20	Uniform	40	16	4.0	130	95°F wet bulb
21	Uniform	20	16	2.5	130	Ambient
22	Uniform	80	20	0	Ambient	Ambient
23	Bottom inlet	40	16	0	Ambient	Ambient
24	Bottom inlet	10	8	1.0	130	Ambient
25	Bottom inlet	10	8	1.0	130	90°F wet bulb
26	Bottom inlet	40	16	4.0	130	Ambient
27	Bottom inlet	20	16	2.5	130	Ambient

Table A.2-3 AP600 PCS Small-Scale Integral Test Matrix (cont.)

Test No.	Steam Outlet	Steam/Air Pressure (psig)	Cooling Air Velocity (ft/sec)	Water Film Flow (gpm)	Cooling Air Temp (°F)	Air Relative Humidity
28	Bottom inlet	30	16	4.0	130	Ambient
29	High inlet	10	8	1.0	130	Ambient
30	High inlet	10	8	1.0	130	95°F wet bulb
31	High inlet	20	16	4.0	130	Ambient
32	High inlet	20	16	4.0	130	95°F wet bulb
33	High water	10	8	1.0	130	Ambient
34	High water	10	8	1.0	130	95°F wet bulb
35	High water	40	16	4.0	130	Ambient
36	High water	20	16	2.5	130	Ambient

Table A.2-4 Large-Scale Heat Transfer Test, Phase 2

Test	Test Number	Description
Pre-operational test	Video recording	Videos of water distribution on top of vessel
	Cold annulus velocity	Low temperature annulus startup velocity
	Water distribution	Calibrate water distribution for three different levels of coverage on the vessel
	Condensate system	Check operation of condensate system
	Velocity sensors	Check operation and determine location of velocity meters for future tests
	Cold helium injection	Inject helium into cold vessel and sample to determine helium distribution at selected time intervals following injection
	Delayed water injection	Provide delayed water distribution flow to the surface of hot vessel and video tape performance
Matrix tests	202.3	Constant vessel pressure
	203.3	Constant high vessel pressure
	213.1	Three steam flow levels with reduced water flow and coverage area
	214.1	Constant steam flow, reduced water flow and coverage area, and variable air cooling flow
	216.1	Constant steam flow with reduced water flow over sections of the vessel
	215.1	Constant steam flow, reduced water flow and coverage area, and variable air cooling flow
	212.1	Three steam flow levels with reduced water flow and coverage area; noncondensable gas samples taken
	217.1	Constant steam flow with helium injection; reduced water flow and coverage area
	220.1	Transient blowdown steam flow, reduced water flow and coverage area, noncondensable gas samples taken
	218.1	Constant steam flow with helium injection; reduced water flow and coverage area; each steam flow maintained for about 1 hour and noncondensable measurements taken

Table A.2-4 Large-Scale Heat Transfer Test, Phase 2 (cont.)

Test	Test Number	Description
	219.1	Constant steam flow with helium injection; reduced water flow and coverage area; each steam flow maintained for about 1 hour and noncondensable measurements taken
	221.1	Transient blowdown steam flow with helium addition sampling; reduced water flow and coverage area

a,b,c

Figure A.2-1 Radial Section Showing Air Path Boundaries Through the Test Model

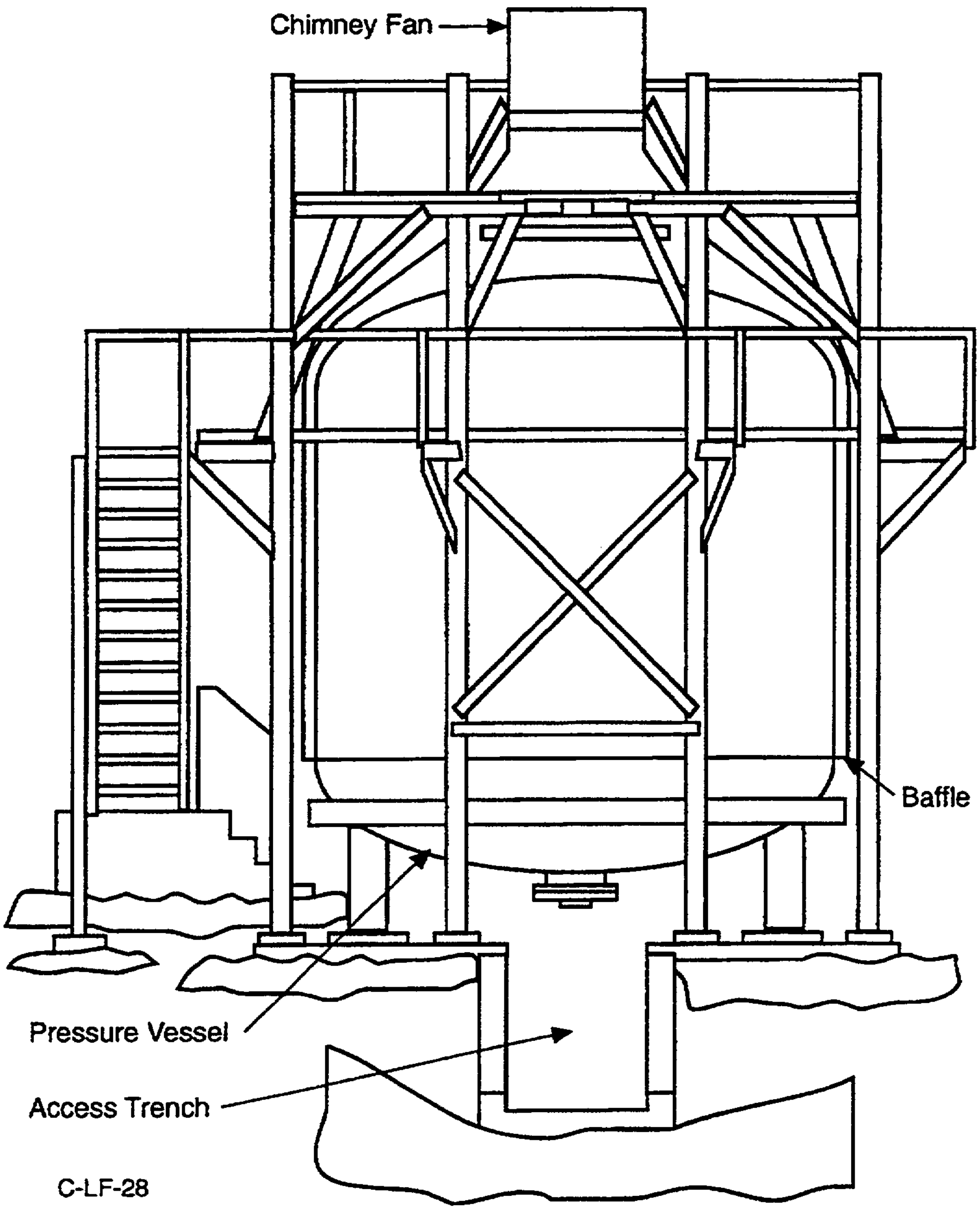

Figure A.2-2 Large-Scale PCS Test Facility

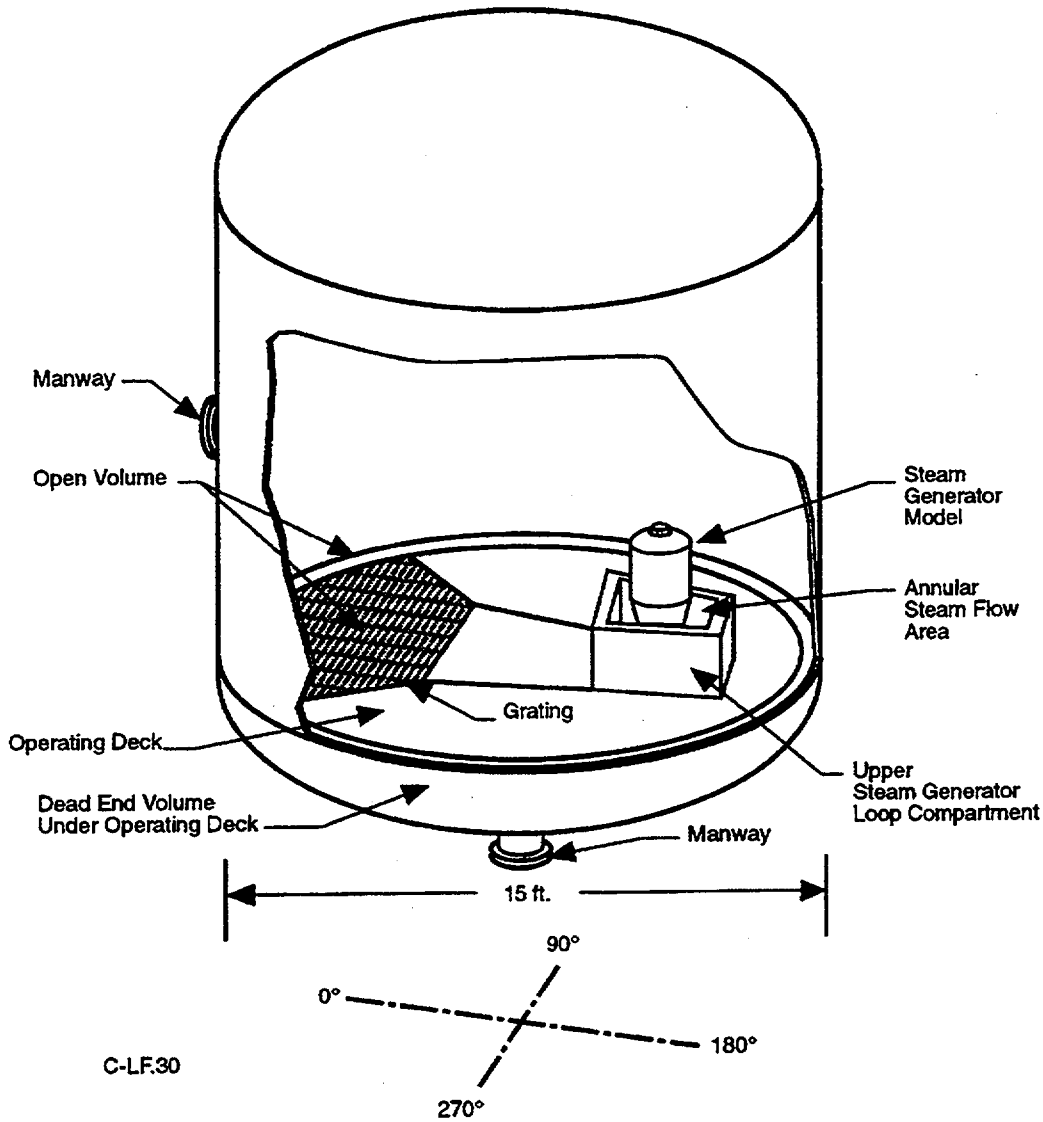

Figure A.2-3 Large-Scale PCS Test Facility

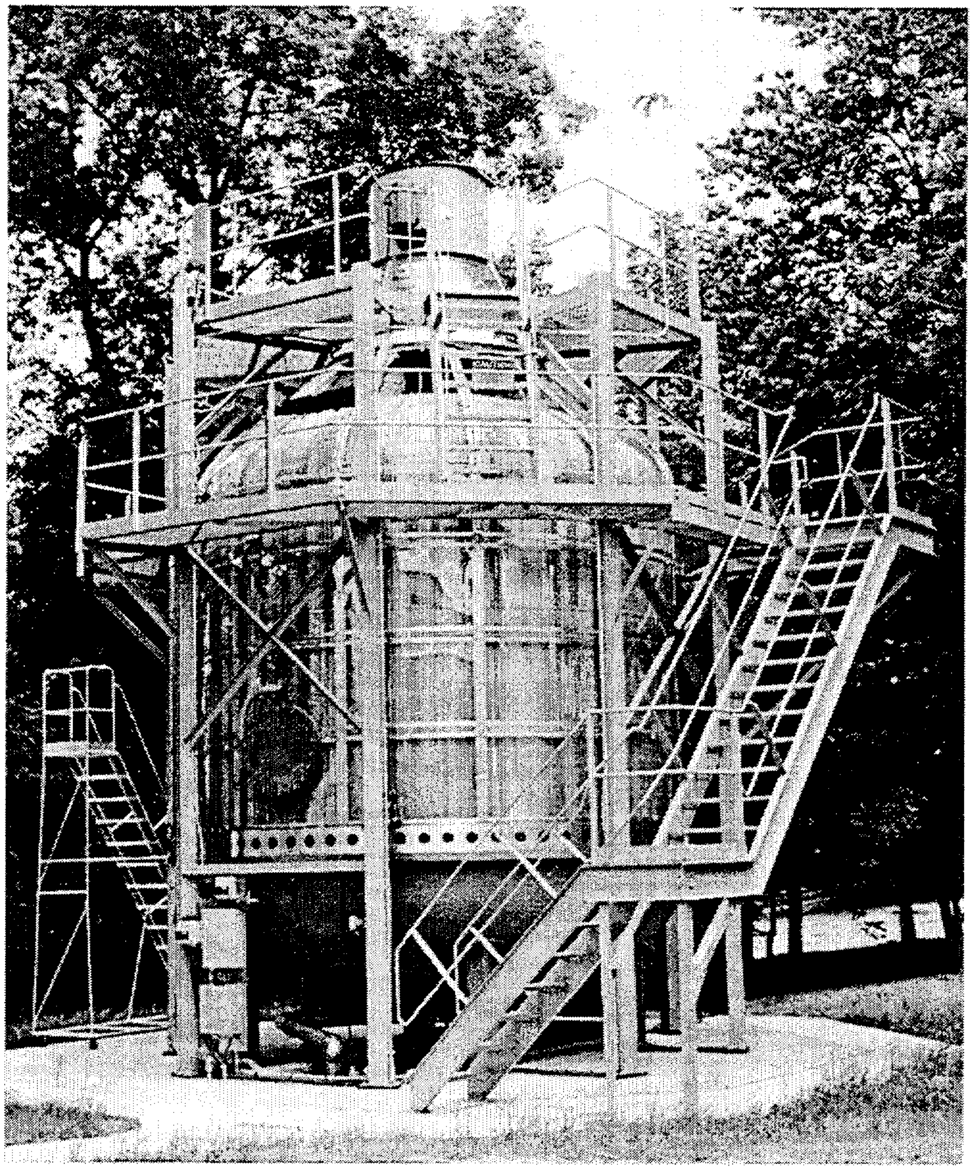

Figure A.2-4 Large-Scale PCS Test Facility

A.3 EQUIPMENT DESIGN VERIFICATION TESTS

The following tests were performed for equipment design verification.

- Normal residual heat removal suction nozzle test (subsection A.3.1)
- RCP/SG channelhead air flow test (subsection A.3.2)
- RCP high-inertia rotor/journal and bearing test (subsection A.3.3)
- In-core instrumentation EMI test (subsection A.3.4)
- Reactor Vessel air-flow visualization test (subsection A.3.5)
- Boron transportation simulation test (subsection A.3.6)
- PXS check valve hydraulic test (subsection A.3.7)
- Operating plant check valve test (subsection A.3.8)

A.3.1 Normal RHR (RNS) Suction Nozzle Test

General Description/Purpose

In order to ensure that the AP600 hot-leg RNS suction nozzle configuration was optimized and that loss of the RHR function during mid-loop operation will not be a concern in the AP600, a series of tests were performed using an existing test facility.

The test model was made of clear plastic material to allow for visual viewing of the water behavior. The model consisted of a simulated reactor vessel with a 1/4.25-scale hot leg and RHR suction pipe. The Froude number was used to scale the test pump flow rates. A void meter and a strip chart recorder were used to measure the percentage of air entrainment by volume in the pump suction piping continuously, and all test runs were recorded on video tape. Two suction nozzle orientations and two potential vortex "breaker" arrangements were tested. For each configuration tested, the critical vortexing water level was measured as a function of both Froude number and loop water level.

Test Matrix/Results

The following configurations were tested:

- A scaled 10-inch RHR pipe in the bottom of the hot leg.

- A "step" nozzle at the bottom of the hot leg and a 10-inch RHR pipe at bottom of the step nozzle. Different diameters (14 to 20 in.) and lengths were investigated for the step nozzle.

These configurations were compared with previous test results obtained with an RHR suction nozzle placed at 45 degrees below the horizontal, the typical configuration on current Westinghouse PWRs.

Among the different nozzle arrangements tested, the optimum arrangement was a step nozzle. As the hot-leg level was further reduced, vortex formation in the hot leg stopped, as water just spilled into and filled the large nozzle. Air entrainment during the "spill" mode was small and would not result in unstable pump/system operation.

A.3.2 RCP SG Channel Head Air-Flow Test

General Description/Purpose

The air-flow test was performed to identify effects on pump performance due to non-uniform channel head flow distribution, pressure losses of the channel head nozzle dam supports and pump suction nozzle, and possible vortices in the channel head induced by the pump impeller rotation.

The air test facility was constructed as an approximate 1/2-scale mockup of the outlet half of the channel head, two pump suction nozzles, and two pump impellers and diffusers. The channel head tubesheet was constructed from clear plastic to allow smoke flow stream patterns to be seen.

Test Matrix/Results

The results of the test confirmed that no adverse flow condition, anomalies, or vortices in the channel head were induced by the dual impellers.

A.3.3 RCP High-Inertia Rotor/Journal and Bearing Tests

General Description/Purpose

An effective way to provide flow during coastdown of a pump during a loss-of-power transient was to add rotational inertia to the pump shaft at a bearing location.

The reference design AP600 canned motor RCP provides a rotating inertia of 5000 lb/ft^2. To achieve this inertia with minimum drag loss, the impeller-end journal contains a 26-inch diameter by 14.5-inch long high-density (depleted uranium alloy) insert. The insert was enclosed in stainless steel for corrosion protection, and the enclosure was hardfaced at the bearing running surfaces for better wear resistance.

The resulting journal diameter was 28 inches, twice the diameter of any previously built water lubricated RCP bearing. Because of the size and unique construction, manufacturing and testing of the journal and bearing assemblies was undertaken. This engineering test program experimentally confirmed theoretical predictions of the parasitic and bearing losses arising from the "high-inertia" rotor concept applied to canned motor pumps. The test program also verified manufacturability and confirmed the adequacy of the design of both the thrust and journal bearings.

One important objective of this effort was to experimentally confirm the theoretical predictions of the parasitic and bearing losses arising from the high-inertia rotor concept applied to canned motor pumps. Theoretical calculations based on empirical drag laws are not sufficiently accurate to permit a final design to be made without accurate experimental verification. The viability of the high-inertia concept depends on limiting the losses to acceptable values. Additional important objectives were to confirm the satisfactory performance of the radial and thrust bearings, and to demonstrate the manufacturability and integrity of a full-scale encapsulated depleted-uranium journal.

In order to measure the losses accurately, a special friction dynamometer was designed, constructed, and put into operation.

Tests of the high inertia RCP were conducted in three phases.

Test Matrix/Results

Phase 1 testing successfully demonstrated the design and construction of a full-scale encapsulated high-inertia journal. Five thousand pounds of depleted-uranium 2-percent molybdenum alloy were cast, machined, encapsulated in stainless steel, precision-clad with hard-facing (Stellite), and balanced at all speeds up to and including 2000 rpm (13 percent overspeed).

The program was completely successful in demonstrating satisfactory performance under load of one of the largest water-lubricated, high-speed pivoted-pad journal bearings ever built. The journal, pivoted-pad radial bearing, thrust bearing, and friction-dynamometer test rig operated smoothly with no significant vibration over the entire speed and load range.

Success was achieved in the accurate measurement of the parasitic drag losses of the complete bearing assembly. These losses were higher than expected. Both radial load and thrust load were shown to have only a minor affect on losses, with speed being the major variable.

The largest contributors to the increase in losses over those originally expected were believed to be the balance cutouts and canopy welds on the journal. Other possible contributors to the losses were identified for investigation in phase 2.

The first objective in phase 2 was to measure the losses with smooth-end covers fitted over the canopy weld and balance cutout areas. The second objective was to determine the affect on the losses by removing the flow plugs blocking the ports of a six-hole centrifugal pump in the rotor. The third objective was to determine the affect on losses by increasing the gap between the outboard end of the motor and the bumper plate.

Smooth-end covers were successfully fabricated and fastened to the canopy weld and balance cutout areas of the high-inertia rotor. However, the resultant loss measurements were higher than those obtained previously in phase 1. Thus, the first try at smoothing these areas was not successful. The phase 2 tests were successful in determining the effect of removing the flow plugs and increasing the axial gap. Neither of these changes produced a large difference in the measured losses. Removal of the bumper plate reduced the losses by about 9 hp. The most significant finding was that there was no difference in measured losses between the two directions of rotation.

Phase 3 tests were performed to investigate a change in the design and location of the radial bearings in order to reduce the drag losses. The design change removed the radial bearing function from the high-inertia rotor and onto the pump shaft. The objective of the current testing was to measure the losses with the radial bearing pads removed and a cylindrical shroud installed to give an annular space with a radial gap of 0.5 inches.

The seven radial bearing pads were removed from the test housing and replaced by a continuous annular space having an average radial clearance of about 0.5 inches. Dynamic analysis predicted that the high-inertia test rotor and shaft would continue to exhibit stable operation. The testing verified the prediction; the test facility remained stable throughout the full speed range to 1761 rpm. Noncontacting displacement transducers were added to measure the relative radial positions of the rotor and housing. These transducers worked very well to provide information to enable the rotor to be kept well-centered in the housing. The program was completely successful in obtaining a large reduction in power losses with the removal of the radial bearing pads, as predicted prior to testing.

A.3.4 In-Core Instrumentation Electro-Magnetic Interference (EMI) Tests

General Description/Purpose

A test was performed to demonstrate that the system would not be susceptible to EMI from the nearby control rod drive mechanisms (CRDMs). The test was performed by mocking up instrument cables, bringing them into close proximity with an operating CRDM, and measuring the resulting noise induced on simulated flux signals.

Test Matrix/Results

The tests demonstrated that induced currents in the fixed in-core detector (FID) cables were acceptably small compared to the FID signals.

A.3.5 Reactor Vessel Air-Flow Visualization Tests

General Description/Purpose

A 1/9-scale model of the AP600 reactor vessel and the four cold legs was constructed at the University of Tennessee. This model was used to visualize the vessel lower plenum to determine if vortices were present and, if so, the effect on them from surrounding features. The model was designed for flow visualization in the lower plenum, so the flow region from the SG outlet through the core support plate was accurately scaled. This included representations of the cold legs, downcomer, lower plenum, and support plate, including the hot-leg segments and the radial support keys in the downcomer and the vortex suppression ring in the lower plenum. Acrylic plastic was used for the cold legs, reactor vessel, and lower plenum, so flow visualization techniques could be employed in these areas. Flow in the model was provided by a blower that exhausted air vertically from the upper plenum region. The flow rate was controlled by a gate valve immediately upstream of the blower. This velocity was measured in each of the four cold legs using low-pressure drop orifices located near the cold leg nozzles.

Test Matrix/Results

These tests confirmed that vortices were effectively eliminated by the design. The absence of adverse effects was confirmed.

A.3.6 Boron Transport Simulation Test

General Description/Purpose

The principal objective of this test program was to simulate the transport of borated water from the SI nozzles to the core inlet region in support of the AP600 reactor design. This information was important when predicting the consequences of any reactivity transients that are terminated by boron injection. The scenario likely to produce the greatest amount of reactivity feedback occurs when one SG was being depressurized to atmospheric pressure. In this case, the loop associated with the faulted SG will have flow driven by natural circulation, while the other loop could be completely stagnant. Gravity-driven SI flow will be initiated as the secondary cooldown reduces the primary system pressure. This scenario could result in a highly asymmetric cooldown of the core and significant reactivity addition until the injected boron migrates to the core.

To determine the characteristics of fluid transport in the reactor, a scaled experiment was performed at the University of Tennessee. For this test program, the reactor was modeled in 1:9 scale. The model included accurate reproductions of the cold legs, downcomer, SI nozzles, vortex suppression ring and secondary core support, lower plenum, and core support plate. Side and top view drawings of the scaled model are shown in Figures A.3-1 and A.3-2. Air was used as the working fluid, with a dense gas serving as the injected fluid. A detailed scaling analysis of the AP600 reactor was performed to determine model flow velocities necessary to accurately model the effects of convection, diffusion, turbulence, and gravity as they apply to fluid transport in the reactor system.

The tests were performed by initially setting a steady-state flow rate in the model reactor vessel, determined by scaling the reactor flow rates. At a known time, injection of the dense gas was triggered. The concentration of the injected gas was measured as a function of time at 24 points immediately downstream of the core support plate.

Test Matrix/Results

The reactor conditions tested represented two different SLB scenarios, as follows:

1) System pressure = 973 psia
Loop 1 flow: 3926.3 gpm @ 432°F
Loop 2 flow: 8021.8 gpm @ 350°F
SI flow: 221.3 gpm @ 132.1°F

2) System pressure = 786 psia
Loop 1 flow: 0.0 gpm
Loop 2 flow: 10226.3 gpm @ 303°F
SI flow: 169.7 gpm @ 123.5°F

Converting these flow rates to reactor system flow velocities allowed scaling to model velocities. As dictated by the scaling report, model velocities were scaled to 0.44, 1.0, and 9.0 times the reactor velocity when using carbon dioxide as the injected gas, while a model velocity of 1.3 times the reactor velocity was used with sulfur hexafluoride. These cases are illustrated in Table A.3-1.

The first four test series simulated the first SLB scenario over the range of model velocities, while the next four series simulated the second scenario. Series 9 was added to provide benchmark data for a case where all loop flows were equal rather than asymmetric. Each test series was composed of five repetitions of six different groupings of gas concentration probe positions, resulting in a total of 30 runs per test series.

The result of averaging the loop and injection flow test data was given in Table A.3-2. For each test series, the expected flow rate and the average achieved flow rate in actual cubic feet per minute are given on the first line of the table box. The second line gives the maximum and minimum flow rates recorded at any time during the five repetitions of each test. The tests results are currently being evaluated.

A.3.7 PXS Check Valve Hydraulic Test

General Description/Purpose

The AP600 PXS uses check valves that operate at low differential pressure during gravity-drain injection. The AP600 PXS line from the containment sump to the reactor vessel injection includes three check valves in series.

The PXS check valve test conducted at the Westinghouse Waltz Mill site used an hydraulic test facility configured to model the AP600 PXS line from the containment sump to the reactor vessel injection connection. The check valve test facility was equipped with two pumps capable of providing a total maximum flow rate of 1000 gpm at about 100 psig discharge head. The pumps were connected to a common discharge header using isolation valves to permit individual or parallel operation, as required, to provide the specific test flow rates. One pump, equipped with a variable frequency drive, was able to satisfy all specified test flow rates (0 to 750 gpm), because of the relatively low-pressure drop associated with the check valves and facility piping.

The test facility also included a flow bypass line, control valves, and metering sections to permit flow control and measurement over the full specified flow. Flow metering sections consisted of calibrated electromagnetic flow meters; 1-inch, 4-inch, and 6-inch flow meters were used to cover the entire specified range of flow rates. The flow meters were installed in parallel vertical metering sections downstream of the check valve test section and in the test section of the loop return line to permit installation of longer lengths of straight pipe upstream.

The check valves were installed between removable piping spool sections of appropriate length to assure fully developed flow upstream and downstream of the check valve test section. The check valve test section was designed to model the AP600 PXS line from the containment sump to the reactor vessel injection connection. The 6-inch valves were installed in series in the main 6-inch line. Flanged connections were provided to permit replacement of each 6-inch check valve with a corresponding length of straight pipe. The 4-inch check valve was installed in a separate 4-inch line that branched into the main 6-inch line via a reducing tee to simulate the proposed plant piping configuration. Isolation valves were provided to permit configuration of the piping to flow through the 4-inch line into the 6-inch line or to bypass the 4-inch line and flow directly through the 6-inch line.

Tests were conducted on individual 4-inch and 6-inch check valves typical of those utilized in the AP600 PXS, with the check valves arranged in various configurations. Pressure taps for measuring differential pressure across the valves were installed. Transparent valve bonnets machined from clear acrylic plate were installed in place of the standard steel bonnets to permit observation and video recording of the valve opening and operational characteristics throughout the range of test flow rates.

Test Matrix/Results

Check valve configurations tested include one 4-inch check valve in series with two 6-inch check valves, two 6-inch check valves in series, and each of two 6-inch check valves individually.

Tests were performed over the range of flow rates between 0 and 750 gpm. Test flow rates were selected to characterize check valve operation when the check valve was fully open and pressure drop was a function of flow velocity, and when the check valve disc position was between fully closed and fully open and pressure drop was a function of the flow area associated with disc position.

The following characteristics were observed during testing and are applicable to each of the tested check valves, whether installed alone or in series:

At lower flow rates, with velocities not sufficient to support the check valve disc beyond 20 percent of the full-open swing, no disc fluctuation was observed.

At higher flow rates, with velocities sufficient to support the check valve disc beyond 20 percent of the full-open swing, but not sufficient to hold the disc in a wide-open position, slight disc fluctuation was observed. The amplitude and frequency of the disc fluctuation were not measured; however, both were sufficiently small that no flow variation was observed, and no valve damage would be expected.

Test flow rates corresponding to the minimum velocities for the tested valves were determined to be about 520 gpm (6.3 ft/sec) for the 4-inch check valve and 510 gpm (7.72 ft/sec) for the 6-inch check valves. At flow rates greater than the minimum value, the valve disc was held in a stable position against the valve stop. At flow rates lower than the minimum value, slight disc fluctuation, as described previously, was observed.

Examination of the check valves at the end of the test program showed no indications of wear.

The NRC staff position on passive failures (SECY 94-084) proposes "to define check valves except for those whose proper function can be demonstrated and documented, in the passive systems as active components subject to single failure consideration." The current PXS arrangement on the IRWST injection lines and the sump recirculation lines meets this position. The AP600 PXS design using simple check valves provides a good design when considering operability (leakage probability/consequences), safety reliability, construction, maintenance, and in-service inspection (ISI)/in-service testing (IST).

Westinghouse has developed an IST plan for AP600 passive system components (including check valves), based on utility input.

A.3.8 Operating Nuclear Plant Check Valve Tests

General Description/Purpose

The AP600 PXS utilizes check valves that operated at low differential pressure during gravity-drain injection. The line from the containment sump to the reactor vessel injection connection includes two 6-inch check valves in series. Tests were conducted at two domestic nuclear power plants to assess the opening performance of check valves after prolonged exposure to reactor coolant system temperature, pressure, and chemistry conditions.

Test Matrix/Results

These tests were conducted to investigate the differential pressure required to open a reactor coolant boundary check valve after a full cycle of operation. The valves tested were 6-inch swing valves typical of those that could be utilized in the AP600 PXS. These tests approximated both normal upstream and downstream pressure and temperature conditions of the check valves. Detailed data on valve opening and flow versus differential pressure was obtained.

Westinghouse modified the AP600 design to incorporate squib valves to reduce the chance of leakage. This change eliminates the differential pressure seen by these check valves during standby operation. As a result, the operating conditions for these check valves is well within the range experienced in operating plants. This testing was not used to support licensing of AP600.

Table A.3-1 Boron Transport Simulation Test Series

Test Series	Loop 1 Cold-Leg Flow Rate (ft^3/min-leg)	Loop 2 Cold-Leg Flow Rate (ft^3/min-leg)	SI Flow Rate (ft^3/min)	SI Gas Species
1	1.48	3.02	0.32	CO_2
2	3.36	6.87	0.74	CO_2
3	4.37	8.93	0.96	SF_6
4	30.26	61.81	6.63	CO_2
5	0.0	3.85	0.25	CO_2
6	0.0	8.76	0.57	CO_2
7	0.0	11.38	0.73	SF_6
8	0.0	78.80	5.09	CO_2
9	39.40	39.40	5.09	CO_2

Table A.3-2 Boron Transport Simulation Test Flow Averages

a,b,c

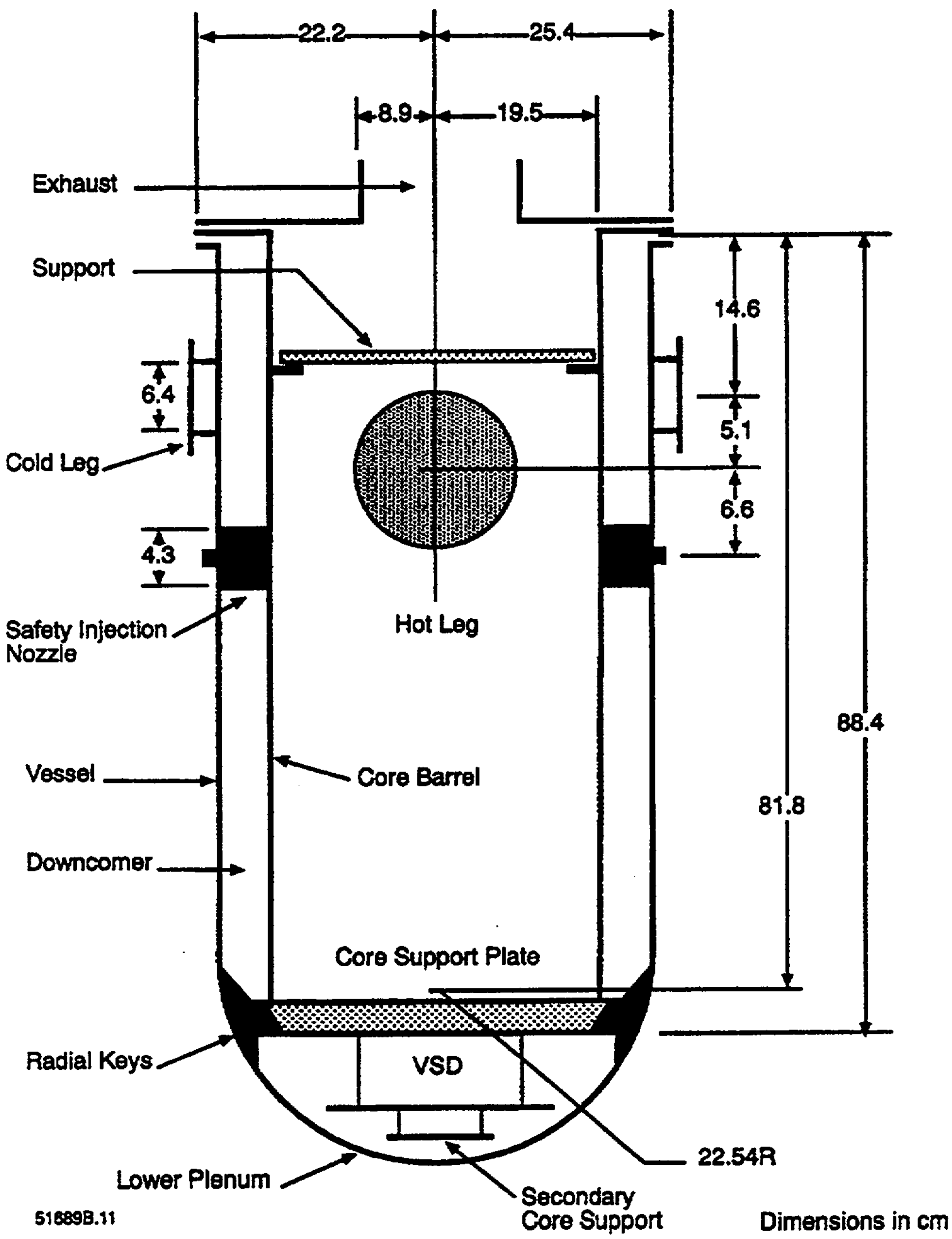

Figure A.3-1 Boron Transport Simulation Test Reactor Vessel Scale Model, Side View

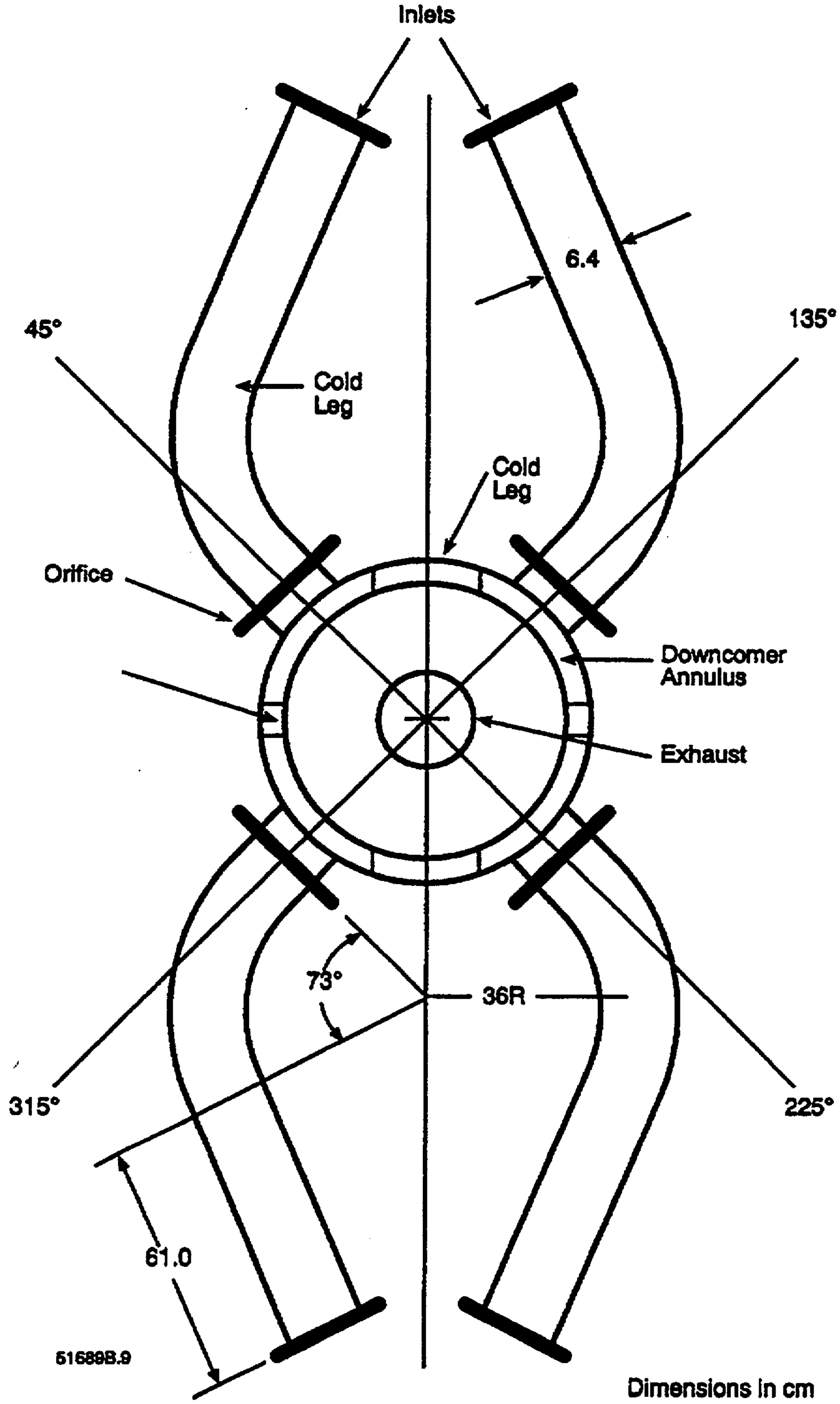

Figure A.3-2 Boron Transport Simulation Test Reactor Scale Model, Top View